

RICE UNIVERSITY

**On the Diffusion and Phase Transitions
of Confined Colloid-Polymer Mixtures**

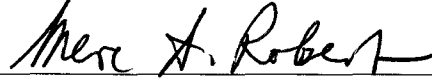
by

Amir Amini

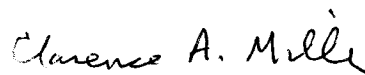
A THESIS SUBMITTED
IN PARTIAL FULFILLMENT OF THE
REQUIREMENTS FOR THE DEGREE

Doctor of Philosophy

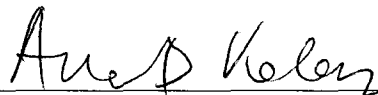
APPROVED, THESIS COMMITTEE:



Marc A. Robert, Chair
Professor of Chemical and Biomolecular
Engineering



Clarence A. Miller
Louis Calder Professor Emeritus of
Chemical and Biomolecular Engineering



Anatoly B. Kolomeisky
Associate Professor of Chemistry

HOUSTON, TEXAS

DECEMBER, 2009

UMI Number: 3421323

All rights reserved

INFORMATION TO ALL USERS

The quality of this reproduction is dependent upon the quality of the copy submitted.

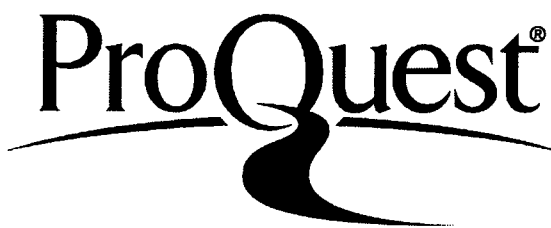
In the unlikely event that the author did not send a complete manuscript and there are missing pages, these will be noted. Also, if material had to be removed, a note will indicate the deletion.



UMI 3421323

Copyright 2010 by ProQuest LLC.

All rights reserved. This edition of the work is protected against unauthorized copying under Title 17, United States Code.



ProQuest LLC
789 East Eisenhower Parkway
P.O. Box 1346
Ann Arbor, MI 48106-1346

Abstract

On the Diffusion and Phase Transitions of Confined Colloid-Polymer Mixtures

by

Amir Amini

Diffusion and phase transitions of confined neutral colloid-polymer mixtures are studied theoretically in one dimension, and theoretically and experimentally in two dimensions.

For colloids in a channel, their short-time self- and collective diffusion coefficients and their long-time mobility are calculated, assuming the colloid-polymer interactions to be of depletion origin and described by the Asakura-Oosawa model. The colloid-polymer mixture is mapped onto an effective one-component system in which the size of the colloids, the hydrodynamic interactions, and the wall effects are taken into account. It is found that depletion interactions reduce the diffusion of colloids for short times and enhance their mobility for long times.

For a single polymer in a colloidal suspension confined to a channel, the self-diffusion coefficient of the polymer center-of-mass is calculated in the ground-state dominance regime as function of suspension density, degree of confinement, and quality solvent quality. The scaling exponents describing the variations of the self-diffusion

coefficient with the degree of polymerization and the radius of the channel are computed. These exponents are found to have higher values than those of a polymer in the absence of colloids. It is also shown that the influence of colloids on polymer diffusion under theta and good solvent conditions is much more pronounced for the latter case.

Monolayers of mixtures of poly(lactic acid) (PLA) and two types of particles, magnetic colloids and Cd-Se nanoparticles, are prepared using the Langmuir-Blodgett technique. Pressure-area isotherms show that the transition from the isotropic phase to the liquid-crystalline smectic-A phase, observed for pure PLA, is suppressed at a critical concentration of the magnetic colloids, whereas it persists in the presence of nanoparticles, even at high concentrations. The theory developed by McMillan for the smectic-A phase in three dimensions is extended to the case of two dimensions, and its predictions are compared to those of the latter as well as to experiment.

Acknowledgements

My twenty years of life as a student comes *formally* to an end with the submission of this thesis. There are many people whose presence has influenced my academic life in one way or another.

I want to start by thanking my parents, to whom I dedicate this thesis. They sacrificed their own future for my education and for my sister's education, guiding us throughout every steps we took in our lives. I would not be in the place where I am now if it was not because of their constant love and support. Then, I would like to thank my sister for her encouragement during difficult times. Her passion and perseverance in life has given me the energy and the joy I needed to pursue my goals.

Next, I should express my deepest gratitude to my adviser, Professor Marc Robert. He has been far more than an academic adviser to me. For me, he is more of an elder brother, a good friend or better, a true role model. Marc has helped me in so many ways during the past five years; not just with my research project but a lot of times with my own personal life. He is and will always be a source of inspiration and enthusiasm for me.

I am indebted to Professor Clarence Miller and Professor Anatoly Kolomeisky who kindly accepted to be members of my thesis committee, to take the time to read my thesis and to share their criticism and comments with me.

Many thanks go to Professor Lisa Biswal for introducing me to the Langmuir-

Blodgett (LB) method, and for the kind permission to use her lab space and equipments. I am grateful to Lisa's graduate students, Kung-Po Chao and Kai-Wei Liu, who patiently trained me on the LB trough and helped me with the experiments.

I have been fortunate to discuss my research with Professor Pierre-Gilles de Gennes and professor Françoise Brochard-Wyart. I am thankful to them for their helpful suggestions and insights. Sadly, professor de Gennes is not among us anymore, but his warmth, openness, and humility are the things that will always stay with me. I am indebted to Professors Ezekiel Cohen, Alan Esker, Patrick Guenoun, David Huse, Dominique Langevin, Athanassios Panagiotopoulos, Jerome Percus, Donald Sullivan, Joseph Straley, and Zhen-Gang Wang for useful discussions and correspondence.

I am thankful to my former groupmates Dr. Juan Carlos Araque and Professor Cheng-Ying Chou for sharing their knowledge and experience. I also want to acknowledge the financial support I received from the National Science Foundation (NSF), the Welch Foundation, and the Kobayashi Fellowship during my entire period as a Ph.D. student.

And, last but not least, I have a huge debt to all the teachers who enlightened me since the beginning of my school years. They are the ones who initially encouraged my curiosity, desire and motivation to learn. I am grateful to my friends and the staff at Rice who made the past five years, with all its ups and downs, exciting and pleasant.

Contents

Abstract	ii
Acknowledgements	iv
List of Figures	vii
Introduction	1
1 Theory of Diffusion	11
1.1 Diffusion in Three Dimensions	11
1.1.1 Collective Diffusion	13
1.1.2 Self-Diffusion	16
1.1.3 Light Scattering and Smoluchowski Dynamics	18
1.1.4 Calculation of the Self-Diffusion Coefficient	20
1.1.5 Calculation of the Collective Diffusion Coefficient	22
1.2 Diffusion in Quasi-One Dimension	24
1.2.1 Screened Hydrodynamic Interactions	26
1.2.2 Concentration Dependence of Self-Diffusion	29
2 Diffusion of Colloids in Confined Colloid-Polymer Mixtures	32
2.1 Mapping to Effective One-Component System	32
2.2 Self-Diffusion and Mobility of Colloids	38
2.3 Results and Discussion	44
3 Diffusion of a Polymer in Confined Colloid-Polymer Mixtures	54
3.1 General Formalism	54
3.2 Polymer in a Θ Solvent - The Gaussian Model	59
3.3 Polymer in a Good Solvent - Swollen Chains	63
3.4 Single Polymer with Many Colloids	66

4	Phase Transitions of Colloid-Polymer Mixtures in Two Dimensions	81
4.1	Materials and Experimental Methods	82
4.2	PLA-Particle Mixtures	88
4.3	McMillan Theory of Smectic-A Phase in Two Dimensions	95
5	Future Studies	103
	Bibliography	107

List of Figures

1	Alternating comb polymers and colloidal particles at an air-water interface.	9
2	Typical pressure-area isotherm for two-dimensional systems.	9
2.1	Confined colloid-polymer mixture in the single-file regime of the colloids.	39
2.2	Depletion zone of polymers in a channel.	39
2.3	Radial distribution function of colloids in a colloid-polymer mixture. .	45
2.4	Short-time self-diffusion coefficient of colloids in solution.	47
2.5	Static structure factor of colloids.	48
2.6	Comparison of the expressions for D_{12}	50
2.7	Short-time gradient diffusion coefficient of colloids.	51
2.8	Long-time mobility factor of colloids.	52
2.9	Mean-squared displacement in one dimension.	53
3.1	Polymer chain confined in a narrow channel.	68
3.2	Dirac delta function barrier potential.	69
3.3	Normalized self-diffusion of an ideal polymer chain.	71
3.4	Normalized self-diffusion of a swollen polymer chain.	72
3.5	Exponent ν in $D \sim N^{-\nu}$	73
3.6	Exponent ω in $D \sim R^\omega$ for an ideal chain.	77
3.7	Exponent ω in $D \sim R^\omega$ for a real chain.	78
3.8	Square-wall barrier potential.	80
4.1	Langmuir-Blodgett trough.	84
4.2	$\pi - A$ isotherms for pure colloidal particles.	86
4.3	$\pi - A$ isotherm for pure PLA molecules.	87
4.4	$\pi - A$ isotherm for mixtures of PLA and magnetic colloids.	90
4.5	$\pi - A$ isotherm for PLA-nanoparticle mixtures at high nanoparticle concentration.	92
4.6	$\pi - A$ isotherm for PLA-nanoparticle mixtures at low PLA concentration.	93
4.7	$\pi - A$ isotherm for PLA-nanoparticle mixtures at fixed nanoparticle concentration.	94
4.8	Order parameters S and σ for $\zeta = 0.5$	100
4.9	Order parameters S and σ for $\zeta = 1.8$	101

Introduction

This thesis is concerned with two problems in the area of colloid-polymer mixtures. The first is diffusion in confined colloid-polymer systems and the second is phase transitions in monolayers consist of colloidal particles and polymer chains.

(A) Diffusion in confined colloid-polymer mixtures

The understanding of the dynamics of complex fluids provides the key to some of the most relevant problems in engineering, physics, chemistry and biology involving for example self-assembling molecular systems, proteins, colloids, cellular filaments, glasses, and membranes. The challenge in studying these systems lies in the fact that the relevant physical processes often occur over a wide range of characteristic length and times scales which can be strongly correlated.

The question of how fluids move through geometrically confined spaces such as pores and channels is also important for understanding a variety of naturally occurring and man-made systems of interest to engineers, physicists, chemists, and biologists. For example, the transport of fluids through carbon nanotubes, porous materials such

as zeolites, and ion channels in biological membranes, is an area of intensive research, and there is a considerable body of literature covering both experimental, theoretical, and computer simulation studies of a wide variety of systems [1].

Among these systems, colloidal suspensions have attracted much attention during the past decade because of their widespread technological applications and the availability of both calibrated model particles and new experimental techniques to study their static and dynamical properties [2].

The use of colloids in technology and medicine is widespread in classical applications including coatings and paints, tires, inks, adhesives, cosmetics, food, and blood. Today, colloids are proving useful in several new technological applications such as colloidal processing of functional ceramics [3], colloidal crystals for photonic bandgap materials [4, 5, 6, 7, 8, 9] and porous metallic nanostructures [10], magnetic colloidal nanoparticles for medical diagnostic [11, 12], colloidal inks for directed assembly of mesoscale periodic structures [13], and colloidosomes for encapsulation [14]. In applications such as coatings and paints, inks, motor oils, biochemical separations processes, detergency, and the processing and preserving of food products, soluble or adsorbing polymers are commonly added to colloidal dispersions. Such polymer additives are instrumental in controlling the stability and rheological properties of colloidal dispersions [15].

The addition of soluble polymer to colloidal dispersions, even in small amounts, has a significant effect on transport properties, mainly because it induces a new type

of interaction between the colloidal particles, the depletion interaction. The depletion interaction is due to the fact that at appropriate concentrations and for suitable ratios of the size of the polymer to that of the colloid for which excluded volume effects become important, an entropic force between the colloidal particles is induced by the presence of the polymer. This entropic force is generally attractive.

When colloid-polymer systems are confined by surfaces, boundary and wall effects become important, and their equilibrium, interfacial and transport properties are expected to differ from those of their bulk three-dimensional counterparts. In quasi one-dimensional geometries, colloidal systems offer practical interest, in particular for diffusion processes in zeolites and microporous solids [16, 17], and in biological systems [18, 19, 20]. In quasi two-dimensional geometries, colloid and colloid-polymer systems also present much interest from the point of view of new applications like the use of two-dimensional protein crystals for immunosensors, highly isoporous ultrafiltration membranes for bioelectronic and biophotonic devices, and thin films [21, 22, 23].

The development of a theory of diffusion in colloid-polymer systems at a fundamental, molecular level, is a problem of great complexity and difficulty. It is indeed known that even for ordinary binary molecular systems much simpler than the colloid-polymer systems studied in this thesis, there is no accurate molecular theory of diffusion for the liquid state, unlike for the gas state. The only available theories are highly approximate hydrodynamic and activated-state models [24]. Consequently, and in order to avoid the introduction of too many uncontrolled approximations,

models of colloid-polymer systems must be developed which are simple enough to be tractable with accuracy.

Previous studies of diffusion have been restricted to pure colloidal systems or to diffusion of polymers in the absence of colloids. Three-dimensional colloidal systems have been investigated over a wide range of concentrations, both by theory [25, 26] and by computer simulations [27, 28], and the cage diffusion concept has proved successful in accounting for experimental results on hard sphere-like colloids [25, 29, 30], as well as in describing diffusion near the colloidal glass transition [31, 32]. Diffusion in one-dimensional colloidal systems has also been studied theoretically and experimentally. It exhibits a noteworthy non-Fickian long-time behavior [33, 34, 35, 36, 37]. Usually, the effects of direct and hydrodynamic interactions on the dynamics of particles is assessed by multiple light scattering experiments in the wavevector and frequency domains. One advantage of colloidal systems is that, in contrast to atomic and molecular fluids, direct observation of the dynamics by light microscopy becomes feasible in real space and real time. This is because the typical relaxation time of particles is of the order of milliseconds, which is orders of magnitude larger than molecular relaxation times (an exception being the special phenomenon of critical slowing down near a critical point). Likewise, the relevant length scale for these structures lies in the mesoscopic rather than molecular range [38].

Diffusion of polymer, in the absence of colloid, has been widely studied in three dimensions [39, 40, 41], and recently results have been reported on two-dimensional

systems, in particular DNA on lipid membranes [42, 43] and polystyrene films [44]. Apart from a theoretical study of diffusion of small colloidal particles in polymer melts [45] and the recent experimental works of our group [46, 47, 48], there appears to be few experimental and no theoretical reports on colloid or polymer diffusion in colloid-polymer systems.

A good starting point to examine the diffusion dynamics of polymers in a colloidal suspension in confined geometries is the Kirkwood formula, which is closely related to the many-body generalized Langevin equation, supplemented by self-consistent field approaches [49]. Experimentally, in order to observe their motion, polymer molecules are tagged with fluorescent probes, and fluorescent microscopy is used to track them.

(B) Phase transitions in monolayers of colloid-polymer mixtures

In contrast to bulk systems, much less is known about the behavior of colloid-polymer systems when they are confined to two dimensions. It is believed [50] that under suitable conditions, these systems phase separate into two coexisting fluid phases, one rich in colloid and the other one rich in polymer. This is similar to what has been observed in the bulk. Mean-field theory predicts that demixing will occur for polymer-to-colloid size ratios greater than 0.32, a result that due to the nature of approximations is inevitably independent of number of dimensions [51]. However, computer simulations reveal that the size ratio corresponding to the onset of phase separation is much greater than the above value and also depends weakly on the col-

loid diameter [52]. Gibbs ensemble Monte Carlo simulations combined with density functional theories, when applied to demixing in colloid-polymer mixtures confined between parallel plates [53], show that the binodal curve moves toward higher polymer activities and lower colloid fugacities, implying capillary condensation of the colloidal liquid in the slit. The effect of confinement between two parallel repulsive walls and the accompanying shift of the critical point has also been investigated by means of grand canonical Monte Carlo simulations [54]. As the distance between the walls increases, the critical exponents gradually change in a non-monotonic fashion from the values of the two-dimensional Ising model to those of the three-dimensional Ising model. There is also experimental evidence for the occurrence of liquid-liquid demixing in colloid-polymer mixtures confined in two-dimensional channels [48]. All these studies share a common feature, that is, the polymer is not totally confined to a plane; in other words, although the motion perpendicular to the walls is restricted, the polymer still retains a three-dimensional conformation and its segments can move out of plane. This, together with the effect of the walls, causes deviations from true two-dimensional behavior.

Nevertheless, it is quite possible to confine the properly chosen colloids and polymers at a liquid-vapor interface (such as an air-water interface), and study their phase behavior using the Langmuir-Blodgett technique. The ability of the Langmuir-Blodgett method to produce thermally and chemically stable polymer monolayers explains its wide use in technological applications, for example in membrane technology,

and in micro-, and nano-electronics. Furthermore, the understanding of the behavior of polymers at interfaces has been significantly stimulated in the past decade due to potential applications in nonlinear optical devices, biosensors and microlithography [55].

Following the pioneering work of Crisp [56, 57] on the polymer poly(methyl methacrylate) (PMMA), the properties of PMMA films, including their stability and hysteresis [58, 59, 60, 61, 62], elasticity [63], and thickness [64, 65], have been studied by using the Langmuir Blodgett method [66, 67], ellipsometry [64], surface light scattering [65], atomic force microscopy [68, 69], and fluorescence spectroscopy [70]. Similarly to polymers, charged and neutral colloids partially wet by water [71, 72] can form monolayers at air-water interfaces, due to surface tension [73], and these monolayers can form various phases depending on their concentration. Lin and Chen [74] have employed enhanced digital video microscopy to study the equilibrium structures of monolayers of sulfate-polystyrene particles at oil-water interfaces, and observed solid, hexatic, and liquid phases.

Clearly, not all colloids and polymers respectively float and lie flat at air-water interfaces. But thanks to several experimental [73, 71, 75, 76, 77], theoretical, and computer simulation studies [78, 79, 80] of colloid and polymer interactions and monolayer stability, it is now possible to create well-characterized monolayers of either colloids or polymers at air-water interfaces.

When a polymer does not spontaneously form a monolayer by itself at the air-water

interface, it is nevertheless sometimes possible to obtain a monolayer by chemical modification. For instance, monolayers of poly(imide) [81] and poly(arylenevinylene) [82] were prepared using the Langmuir-Blodgett method by attaching hydrophobic chains to the precursor polymers. Another class of such polymers, comblike polymers such as copolymers derived from maleic acid and maleic anhydride, has drawn much attention [83]. These polymers can be considered the polymeric analogue of low-molecular weight amphiphilic molecules. While their backbone is typically hydrophilic, the attached side chains are usually chosen to be hydrophobic in order to keep the water-soluble backbone at the air-water interface. This enables one to change the conformation of these polymers at the interface simply by changing the degree of hydrophobicity by using different side chains. Nieuwkerk et al. [84] reported the formation of hydrophobically-modified maleic anhydride and maleic acid copolymers on several subphases. In general, at low concentrations, the side chains lie on the air-water interface, whereas at sufficiently high concentrations (semi-dilute regime), the side chains tend to lie upwards [83].

A schematic of this situation together with the associated isotherm is depicted in Fig.1 and Fig.2. The isotherm exhibits a first-order phase transition from a liquid expanded (LE) state with no orientational order to a liquid-condensed (LC) state possessing orientational order in the side chains. Pressure-area isotherms and Brewster-angle microscopy confirm the formation of a monolayer in these systems, which upon compression eventually turns into a multilayer and ultimately into a solid.

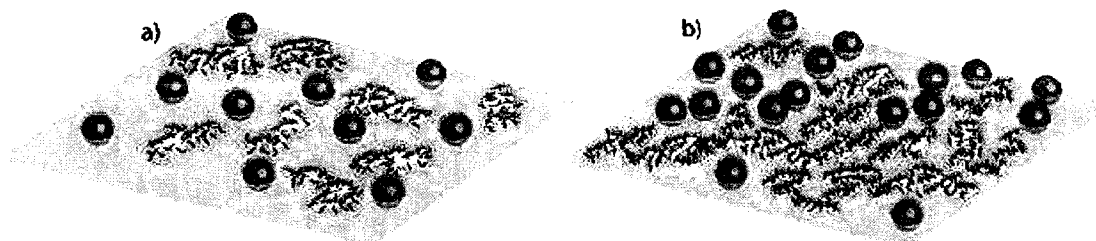


Figure 1: Alternating comb polymers and colloidal particles at an air-water interface: a) dilute regime, where the side chains lie flat on the interface; b) concentrated regime, where the side chains stand up.

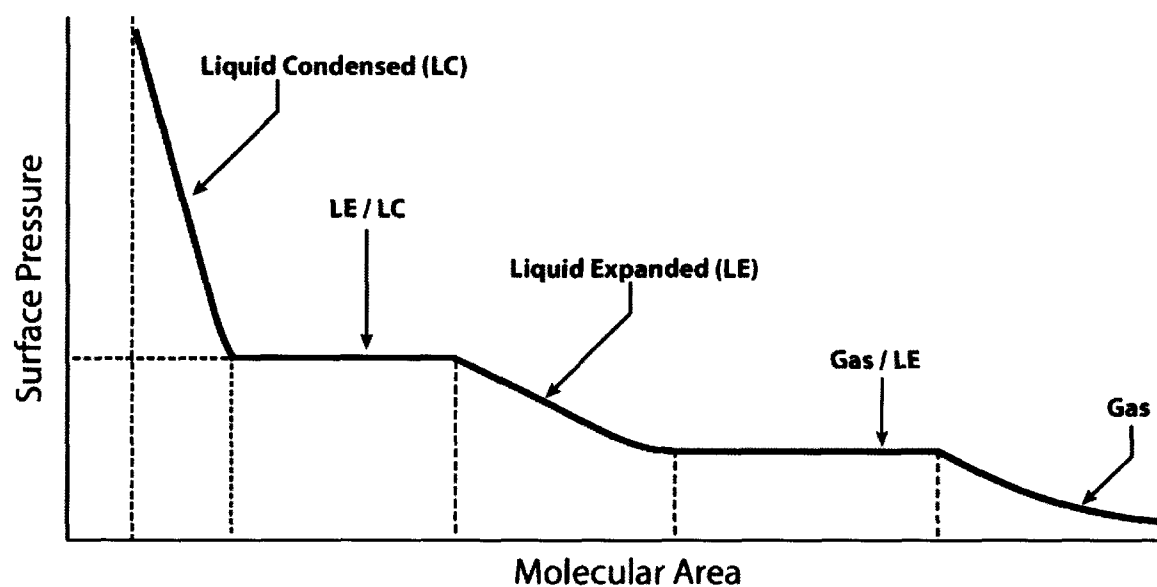


Figure 2: Typical Pressure-area isotherm for two-dimensional systems which exhibit a first-order transition, using the Langmuir-Blodgett method.

This thesis is organized as follows. Chapter 1 presents a brief background on the fundamentals of diffusion processes and the theoretical foundations of the dynamics of interacting many-body systems from a microscopic point of view. Chapters 2 and 3 deal with the models and methodologies employed to determine the diffusion coefficients of polymer and colloid in a confined colloid-polymer mixture, as a function of colloid and polymer concentrations, of their sizes, and of the confinement geometry. Chapter 4 describes the phase transitions observed in a colloid-polymer mixture using the Langmuir-Blodgett technique and examines the implications of a mean-field theory on the results.

Chapter 1

Theory of Diffusion

1.1 Diffusion in Three Dimensions

The dynamics of colloidal suspensions can be discussed on several levels of description, depending on the time scale and the associated length scale of interest. The most detailed description is provided by the deterministic Liouville dynamics, which includes the microscopic time evolution of all degrees of freedom, i.e., the positions and momenta of colloidal particles and solvent molecules. However, such a detailed description is not needed when one is merely interested in the slow dynamics of the colloidal particles, since these are substantially larger and heavier than the small solvent molecules. Thus it is possible to average out the fast fluctuations in the solvent particles' positions and momenta. This leads to a coarse-grained level of description, valid for times much longer than the relaxation time of the solvent molecules

($t \gg \tau_s \approx 10^{-12}s$), in which only the phase space variables of the colloidal particles appear explicitly. At this level, the solvent is reduced to a Navier-Stokes fluid exerting hydrodynamic friction forces on the colloidal particles. The only remnant of the averaged fast degrees of freedom are the Gaussian stochastic forces driving the irregular Brownian motion of the particles [85].

Two types of diffusion processes are to be distinguished: *collective* and *self-diffusion*. Collective (cooperative) diffusion relates to the simultaneous motion of many Brownian particles, induced by the density gradients of these particles, while self-diffusion concerns the dynamics of a single Brownian particle under the influence of interactions with surrounding Brownian particles in a system with homogeneous densities of constituents. The single particle under consideration is commonly referred to as the *tracer particle* or the *tagged particle*, while the remaining Brownian particles are referred to as host particles [86].

To further elucidate the difference between these two types of diffusion processes, we note that in collective diffusion *all particles* participate in the relaxation of concentration fluctuations towards equilibrium (cooperative motion). This is the case for experimental studies of macroscopic systems where two sub-systems with concentrations $c + \delta c$ and $c - \delta c$ are brought into contact, and the concentration profile is monitored as a function of time. Thus cooperative diffusion reflects the speed at which non-uniformities in particle concentration propagate through the system. On the other hand, if for example a small fraction of the particles is radioactive (tagged

particles), we can see them spread out with a certain self-diffusion coefficient which is in general completely different from the collective diffusion coefficient (both diffusion coefficients coincide only in dilute solutions) [49].

1.1.1 Collective Diffusion

Let $\rho(r, t)$ denote the space- and time-dependent macroscopic density of the Brownian particles, and $\mathbf{J}(r, t)$ their flux. Then the continuity equation, which expresses conservation of the number of Brownian particles, reads

$$\frac{\partial}{\partial t} \rho(r, t) = -\nabla \cdot \mathbf{J}(r, t). \quad (1.1)$$

In the case of collective diffusion, the flux is driven by gradients in the density of Brownian particles. For small gradients, the flux can formally be written as

$$\mathbf{J}(r, t) = - \int d\mathbf{r}' \int dt' D(\mathbf{r} - \mathbf{r}', t - t') \nabla' \rho(\mathbf{r}', t'), \quad (1.2)$$

where $D(\mathbf{r}, t)$ is the diffusion kernel, which vanishes for $t < 0$. To leading order in density gradients and for otherwise translationally invariant systems, the diffusion coefficient is a function of \mathbf{r} and \mathbf{r}' only through the difference $\mathbf{r} - \mathbf{r}'$. When the current flux at a point \mathbf{r} is fully determined by the instantaneous density gradient at the *same* point, so that there is no coupling with gradients in adjacent points and with preceding states of the system, the diffusion kernel is proportional to a delta distribution in both position and time, that is, $D(\mathbf{r} - \mathbf{r}') = D(\mathbf{r}, t) \delta(\mathbf{r} - \mathbf{r}') \delta(t - t')$, so that $J(\mathbf{r}, t) = -D(r, t) \nabla \rho(\mathbf{r}, t)$. In general, however, there is a coupling between

gradients in density at different positions due to interactions between the Brownian particles. Also, the evolution at a certain instant of time may depend on states at earlier times.

In the absence of such memory effects, we thus have, as noted above,

$$D(\mathbf{r} - \mathbf{r}', t - t') = D(\mathbf{r} - \mathbf{r}', t)\delta(t - t') , \quad (1.3)$$

and the current density \mathbf{J} is fully determined by the instantaneous density profile

$$\mathbf{J}(\mathbf{r}, t) = - \int d\mathbf{r}' D(\mathbf{r} - \mathbf{r}', t) \nabla' \rho(\mathbf{r}', t) . \quad (1.4)$$

Substitution of Eq.(1.3) into Eq.(1.2) and Fourier transformation with respect to position yields

$$\frac{\partial}{\partial t} \rho(\mathbf{k}, t) = -D(\mathbf{k}, t) k^2 \rho(\mathbf{k}, t) . \quad (1.5)$$

The solution of Eq.(1.5) is

$$\rho(\mathbf{k}, t) = \rho(\mathbf{k}, 0) \exp[-D_c(\mathbf{k}, t) k^2 t] , \quad (1.6)$$

where the collective diffusion coefficient is defined as

$$D_c(\mathbf{k}, t) = \frac{1}{t} \int_0^t dt' D(\mathbf{k}, t') . \quad (1.7)$$

For isotropic systems, the collective diffusion coefficient is only a function of $k = |\mathbf{k}|$. The zero-wavevector limit of the collective diffusion coefficient is called the *gradient diffusion coefficient*, D_∇ , which describes transport of Brownian particles in a density profile with a constant gradient. Hence

$$\lim_{k \rightarrow 0} D_c(k, t) = D_\nabla . \quad (1.8)$$

The limit in Eq.(1.8) should be interpreted as: “take k so small that gradients in the density may be considered constant over distances equal to the range of the interaction between the Brownian particles.” Also, the form of the density profile remains the same, since only very long-wavelength density waves are present during the entire relaxation of smooth gradients. Therefore, the time dependence of the diffusion coefficient is lost. We are thus led to the following conjecture [86]:

The collective diffusion coefficient is independent of time for small wavevectors.

Short-Time and Long-Time Collective Diffusion

The initial decay of a purely sinusoidal density profile is described by the collective diffusion coefficient in Eq.(1.7) for small times, which is referred to as the (wavevector-dependent) short-time collective diffusion coefficient $D_c^s(k)$

$$D_c^s(k) = \lim_{t \rightarrow 0} D_c(k, t) . \quad (1.9)$$

In practice, the short-time limit is reached for times of order $\tau_B = m/\zeta_0 \sim 1ns$, where τ_B is the Brownian time in which the initial velocity of a particle of mass m relaxes to equilibrium, and $\zeta_0 = 6\pi\eta_s a$ is the friction coefficient of an isolated spherical particle of radius a in a solvent of viscosity η_s . The late stage decay of the Fourier component of a density profile that was originally purely sinusoidal with wavelength $\lambda = 2\pi/k$, is described by the long-time collective diffusion coefficient $D_c^l(k)$

$$D_c^l(k) = \lim_{t \rightarrow \infty} D_c(k, t) . \quad (1.10)$$

1.1.2 Self-Diffusion

The simplest quantity that characterizes the motion of a single Brownian particle is its mean-squared displacement $W(t)$, defined as

$$W(t) = \langle |\mathbf{r}(t) - \mathbf{r}(0)|^2 \rangle, \quad (1.11)$$

where $\mathbf{r}(t)$ is the position vector of the tracer particle at time t . For $\tau_B \sim t \ll \tau_p$ and for $t \gg \tau_p$ ¹ [86], $W(t)$ is linear in time and is given by

$$W(t) = 6D_s(t)t, \quad (1.12)$$

where D_s is the time-dependent self-diffusion coefficient, and $\tau_p = a^2/D_0 \sim 1ms$ is the Péclet time characteristic for free particle diffusion over a distance equal to its own radius, with $D_0 = k_B T/\zeta_0$ the diffusion coefficient of a single particle at infinite dilution. To make connection with light scattering experiments, the above definition of the self-diffusion coefficient, as we shall see in the next section, is generalized to a time- and wavevector-dependent coefficient $D_s(\mathbf{k}, t)$, in analogy with its collective counterpart. However, most of the time we are interested in the $k \rightarrow 0$ limit, because it identifies the macroscopic self-diffusion as well as $W(t)$.

Short-Time and Long-Time Self-Diffusion

On average, the tracer particle resides at positions where the “free energy landscape” set up by host particles exhibits minima. Short-time diffusion of the tracer

¹For particles interacting via long-range forces, τ_p , in these relations, has to be replaced by the interaction time τ_I (see Eq.(1.15)).

particle thus relates to its displacements away from such minima. The diffusive motion away from the free energy minima is characterized by the short-time self-diffusion coefficient $D_s^s(k)$

$$D_s^s(k) = \lim_{t \rightarrow 0} D_s(k, t) . \quad (1.13)$$

The initial mean-square displacement is related to the zero-wavevector limit of $D_s^s(k)$ (macroscopic self-diffusion coefficient)

$$\lim_{t \rightarrow 0} W(t) = 6D_s^s(k=0)t . \quad (1.14)$$

For later times, the tracer particle climbs over free energy barriers, which changes the time-dependence of the mean-squared displacement, and the self-diffusion coefficient may then become time-dependent. However, for long times $t \gg \tau_I$, when the tracer particle has crossed many free energy barriers, the mean-square displacement is again proportional to t . Here

$$\tau_I = 1/D_c^l(k_m)k_m^2 \quad (1.15)$$

is the interaction time and k_m is the wavevector at which the static structure factor attains its maximum. The right-hand side of Eq.(1.15) is approximately the time that it takes a density wave of wavelength λ_m to fully relax. In the case of particles interacting via short-range forces, the long-time limit is reached when $t \gg \tau_p$. The corresponding diffusion coefficient in this case is the long-time diffusion coefficient $D_s^l(k)$

$$D_s^l(k) = \lim_{t \rightarrow \infty} D_s(k, t) , \quad (1.16)$$

and

$$\lim_{t \rightarrow \infty} W(t) = 6D_s^l(k=0)t. \quad (1.17)$$

1.1.3 Light Scattering and Smoluchowski Dynamics

The main experimental tools to investigate the statics and dynamics of colloidal suspensions are static and dynamic light scattering. Hence, most theoretical work has been devoted to a quantitative understanding of light scattering data in terms of mesoscopic properties of the suspended particles [85]. A dynamic light scattering experiment on a monodisperse system measures the collective diffusion coefficient for a wavevector that is set by the scattering angle

$$S(q, t) = S(q)\exp[-D_c(q, t)q^2t], \quad (1.18)$$

where

$$S(q, t) = \frac{1}{N} \sum_{i,j=1}^N \langle \exp\{i\mathbf{q} \cdot [\mathbf{r}_i(t) - \mathbf{r}_j(0)]\} \rangle \quad (1.19)$$

is the collective dynamic structure factor ² measured in dynamic light scattering experiments, with $S(q)$ the static structure factor, which can be measured in a static light scattering experiment, and $q = \frac{4\pi}{\lambda} \sin(\theta/2)$ is the momentum-transfer vector. The angular brackets $\langle \rangle$ denote the equilibrium ensemble average in the canonical ensemble. Similarly, the self-diffusion coefficient can be obtained by dynamic light scattering experiments at large q 's, and is related to the self dynamic structure factor

²Some authors call this the collective intermediate scattering function $F(k, t)$, and reserve the term collective dynamic structure factor for its Fourier transform $S(k, \omega)$.

³ by

$$S_s(q, t) = \exp[-D_s(q, t)q^2t]. \quad (1.20)$$

Since dynamic light scattering experiments are restricted to correlation times $t \geq 10^{-6}s$, which are usually orders of magnitude larger than τ_B , one only observes a much slower equilibration of the Brownian particles' positions. This allows for a coarse-grained configuration-space description of the relaxation of spatial coordinates for times and distances much larger than τ_B and $(D_0\tau_B)^{1/2}$ respectively (Smoluchowski dynamics). Within the framework of Smoluchowski dynamics, the time evolution of the system of N interacting particles is given by [87]

$$\frac{\partial}{\partial t}p(\mathbf{r}^N, t) = \hat{\Omega}p(\mathbf{r}^N, t), \quad (1.21)$$

where p is the probability of finding the particles at \mathbf{r}^N at time t and $\hat{\Omega}$ is the Smoluchowski operator defined by

$$\hat{\Omega} = \sum_{i,j=1}^N \nabla_i \cdot \mathbf{D}_{ij}(\mathbf{r}^N) \cdot [\beta \nabla_j U(\mathbf{r}^N) + \nabla_j]. \quad (1.22)$$

Here $\nabla_i = \partial/\partial \mathbf{r}_i$, $\beta = 1/k_B T$, and \mathbf{D}_{ij} is the diffusion tensor which incorporates the hydrodynamic interactions. The time correlation of two arbitrary phase functions can be expressed in terms of this operator. Most importantly, collective and self dynamic structure factors are given by [88]

$$S(k, t) = \frac{1}{N} \langle \delta n(-\mathbf{k}) e^{\hat{\Omega}_B t} \delta n(\mathbf{k}) \rangle \quad (1.23)$$

³Like its collective counterpart, this is sometimes called the self intermediate scattering function $F_s(k, t)$, and the term self dynamic structure factor is reserved for its Fourier transform $S_s(k, \omega)$.

$$S_s(k, t) = \langle \delta n_1(-\mathbf{k}) e^{\hat{\Omega}_B t} \delta n_1(\mathbf{k}) \rangle, \quad (1.24)$$

where $\delta n(\mathbf{k})$ is a plane-wave collective density fluctuation mode with wavevector \mathbf{k} , i.e.,

$$\delta n(-\mathbf{k}) = \sum_{i=1}^N e^{-i\mathbf{k}\cdot\mathbf{r}_i} - \langle \sum_{i=1}^N e^{-i\mathbf{k}\cdot\mathbf{r}_i} \rangle, \quad (1.25)$$

and $\delta n_1(\mathbf{k})$ is the one-particle density fluctuation mode, i.e.,

$$\delta n(-\mathbf{k}) = e^{-i\mathbf{k}\cdot\mathbf{r}_1} - \langle e^{-i\mathbf{k}\cdot\mathbf{r}_1} \rangle. \quad (1.26)$$

$\hat{\Omega}_B = \hat{\Omega}^\dagger$ is the backward (adjoint) Smoluchowski operator describing the time evolution of the system, i.e.,

$$\hat{\Omega}_B = \hat{\Omega}^\dagger = \sum_{i,j=1}^N [\nabla_i - \beta \nabla_i U(\mathbf{r}^N)] \cdot \mathbf{D}_{ij}(\mathbf{r}^N) \cdot \nabla_j. \quad (1.27)$$

1.1.4 Calculation of the Self-Diffusion Coefficient

The experimentally determined behavior of the mean-squared displacement can be quantitatively described within the Smoluchowski dynamics, which allows one to relate the diffusion coefficient to the effective interparticle forces. This is achieved by using the conserved one-particle density as the slow variable in the Mori-Zwanzig projection operator formalism [89]. From this choice of slow variables follows the time evolution equation for the self dynamic structure factor [90] (also called the van Hove self-correlation function and denoted $G(q, t)$)

$$\frac{\partial}{\partial t} S_s(q, t) = -q^2 D_s^s S_s(q, t) + \int_0^t du M_s(q, t-u) S_s(q, u), \quad (1.28)$$

in which $M_s(q, t)$ is the self memory function. The short-time self-diffusion coefficient is easily shown to be given by[91]

$$D_s^s = \langle \hat{q} \cdot \mathbf{D}_{11}(\mathbf{r}^N) \cdot \hat{q} \rangle_{\text{eq}} . \quad (1.29)$$

The exact calculation of D_s^s is not feasible, due to the complicated many-body character of hydrodynamic interactions. However, at the two-particle level, series expansions of D_{11} in powers of (a/r) are known, in principle, to arbitrary order. These expansions have the form [92]

$$\mathbf{D}_{11}(\mathbf{r}^N) = D_0 \left\{ \mathbf{1} + \sum_{j=2}^N [A_s(r_{1j}) \hat{r}_{1j} \hat{r}_{1j} + B_s(r_{1j}) (\mathbf{1} - \hat{r}_{1j} \hat{r}_{1j})] \right\} , \quad (1.30)$$

where the self-mobility functions up to order $(a/r)^8$ are given by

$$A_s(r_{1j}) = -\frac{15}{4} \left(\frac{a}{r_{1j}} \right)^4 + \frac{11}{2} \left(\frac{a}{r_{1j}} \right)^6 \quad (1.31)$$

$$B_s(r_{1j}) = -\frac{17}{16} \left(\frac{a}{r_{1j}} \right)^6 . \quad (1.32)$$

The memory kernel $M_s(q, t)$ can be written as an autocorrelation function of reduced one-particle forces. It contains the effect of interparticle forces on the self-diffusion, and is expected to decay faster than $S_s(q, t)$.

An exact calculation of the memory function is possible only in a few limiting cases. However, various approximations of $M_s(q, t)$ at different levels of sophistication have been discussed in the literature [93, 94]. With $M_s(q, t)$ in hand, the long-time wavenumber-dependent self-diffusion coefficient can be obtained from [88]

$$D_s^l(k) = 1 / \int_0^\infty dt k^2 S_s(k, t) . \quad (1.33)$$

1.1.5 Calculation of the Collective Diffusion Coefficient

Information on the collective diffusion coefficient is contained in the dynamic light scattering data of $S(q, t)$. It is possible to explain all the experimentally observed features of $S(q, t)$, in particular the generally non-exponential decay, the wavenumber-dependent D_c , and to some extent the equality of short-time and long-time collective diffusion coefficients in the long-wavelength limit, by using the generalized Smoluchowski equation as the underlying transport equation in the Mori-Zwanzig projection operator formalism [95]. In the case of collective diffusion, it is appropriate to choose the Fourier components of the microscopic density fluctuations as the slow variables in the projection operator formalism. This choice leads to the following memory equation for the dynamic structure factor [90]

$$\frac{\partial}{\partial t} S(q, t) = -q^2 D_{eff}(q) S(q, t) + \int_0^t du M(q, t-u) \frac{S(q, u)}{S(q)}, \quad (1.34)$$

which is valid for times $t \gg \tau_B$. Here $D_{eff}(q)$ is given by the ratio

$$D_{eff}(q) = D_0 \frac{H(q)}{S(q)}, \quad (1.35)$$

where $H(q)$ is the hydrodynamic function

$$H(q) = \frac{1}{N} \left\langle \sum_{i,j=1}^N \hat{\mathbf{q}} \cdot \frac{\mathbf{D}_{ij}(\mathbf{r}^N)}{D_0} \cdot \hat{\mathbf{q}} e^{i\mathbf{q} \cdot (\mathbf{r}_i - \mathbf{r}_j)} \right\rangle, \quad (1.36)$$

which is positive definite due to the positive definiteness of the super-matrix of many-body diffusion tensors \mathbf{D}_{ij} . The general form of $D_{ij}(i \neq j)$ at the two-particle level is [86]

$$\mathbf{D}_{ij} = D_0 \{ A_c(r_{ij}) \hat{\mathbf{r}}_{ij} \hat{\mathbf{r}}_{ij} + B_c(r_{ij}) [\mathbf{1} - \hat{\mathbf{r}}_{ij} \hat{\mathbf{r}}_{ij}] \}, \quad i \neq j, \quad (1.37)$$

where the cross-mobility functions up to order $(a/r)^9$ are given by

$$A_c = \frac{3}{2} \frac{a}{r_{ij}} - \left(\frac{a}{r_{ij}} \right)^3 + \frac{75}{4} \left(\frac{a}{r_{ij}} \right)^7 \quad (1.38)$$

$$B_c = \frac{3}{4} \frac{a}{r_{ij}} + \frac{1}{2} \left(\frac{a}{r_{ij}} \right)^3. \quad (1.39)$$

The hydrodynamic function contains the configuration-averaged effect of hydrodynamic interactions on the short-time dynamics. The collective memory function $M(q, t)$, which is expected to decay faster than $S(q, t)$, is responsible for the deviations from a single-exponential decay of $S(q, t)$ for times $t \gtrsim \tau_I$. Knowing $M(q, t)$, which is expressible as an autocorrelation function of the collective random force, the long-time wavenumber-dependent collective diffusion coefficient can be obtained from [88]

$$D_c^l(k, t) = S(k) / \int_0^\infty dt k^2 S(k, t). \quad (1.40)$$

In suspensions of interacting particles, a single exponential decay of $S(q, t)$ is observed only in two limiting cases: firstly, at short times, and secondly, in the hydrodynamic regime of very small wave numbers q and long times $t \gg \tau_I$. At short times, as has already been seen, one finds an exponential decay with the first cumulant given by $\Gamma^1(q) = q^2 D_{eff}(q)$. The effective diffusion coefficient reduces for $q \ll q_m$ to the macroscopic short-time collective diffusion coefficient, i.e., $D_c^s = \lim_{q \rightarrow 0} D_{eff}(q)$. In systems with strong repulsive pair forces, D_c^s is found, at finite concentrations, to be substantially larger than the free particle diffusion coefficient D_0 . In the opposite limit of $q \gg q_m$, D_{eff} becomes again independent of q , and reduces to D_c^s . For long

times, macroscopic isothermal gradient diffusion close to equilibrium can be described by the phenomenological diffusion equation

$$\frac{\partial}{\partial t} \rho_{\mathbf{q}}(t) = -q^2 D_c^l \rho_{\mathbf{q}}(t), \quad (1.41)$$

where $\rho_{\mathbf{q}}(t)$ is the Fourier component of $\rho(\mathbf{r}, t)$. According to Onsager's regression hypothesis [96, 97], the density autocorrelation function is expected to obey, in the hydrodynamic limit, the same evolution equation as $\rho_{\mathbf{q}}(t)$. This implies at once

$$\lim_{t \rightarrow \infty} \lim_{q \rightarrow 0} \frac{S(q, t)}{S(q)} = \exp(-q^2 D_c^l t), \quad (1.42)$$

and therefore, D_c^l is measurable also with dynamic light scattering performed in the limit $q \ll q_m \sim (D_0 \tau_I)^{-1/2}$ and $t \gg \tau_I$, with $q^2 t$ held fixed at a value of $\mathcal{O}(1)$. The limit $q \rightarrow 0$ also implies the thermodynamic limit, which needs to be taken first.

1.2 Diffusion in Quasi-One Dimension

The unique feature that distinguishes quasi-one-dimensional diffusion from diffusion in higher dimensions is the geometric confinement that forces the particles into a single file with a fixed spatial sequence. This confinement generates a self-diffusion mechanism that has a different time-dependence of the mean-squared particle displacement in different time domains. For time intervals shorter than the time between particle collisions, in the presence of a randomizing background fluid, the probability density for particle displacement is

$$P_S(x, t) = (4\pi D_s^3 t)^{-\frac{1}{2}} \exp\left[-\frac{x(t)^2}{4D_s^3 t}\right]. \quad (1.43)$$

However, excluding the mutual passage of particles severely restricts the probability for large single particle displacements, and therefore drastically reduces the diffusion rate at long times (anomalous diffusion) [98]. An analytic description of one-dimensional diffusion in system of hard rods with stochastic background forces, neglecting hydrodynamic interactions, was first reported by Harris [99]. Several other one-dimensional systems have been examined with a similar approach [100, 101]; the results obtained are in mutual agreement. For an infinite one-dimensional system, the long-time behavior of the probability density for displacement x is [102]

$$P_L(x, t) = (4\pi Ft^{1/2})^{-\frac{1}{2}} \exp \left[-\frac{x(t)^2}{4Ft^{1/2}} \right], \quad (1.44)$$

where F is the mobility coefficient defined by

$$F = F^{HR} = l \sqrt{\frac{D_0}{\pi}} = \frac{1 - \rho\sigma}{\rho} \sqrt{\frac{D_0}{\pi}} = D_0 \sqrt{\frac{2t_c}{\pi}}. \quad (1.45)$$

F^{HR} denotes the mobility of the hard rods, σ is the particle length (diameter), ρ is the one-dimensional number density, l is the mean spacing between the particles, and $t_c = l^2/2D_0$ is the mean time between collisions. Eq.(1.44) and Eq.(1.45) provide a remarkably simple picture of the one-dimensional diffusion at long times: the self-diffusion process, determined by the width of the probability density, is proportional to $t^{1/2}$, and the proportionality constant is determined by the short-time *individual particle* dynamics

$$\langle x^2(t) \rangle = 2Ft^{1/2}. \quad (1.46)$$

Recently, Kollmann [103] has reported an analysis of the long-time behavior of

one-dimensional diffusion that is valid for both atomic and colloid systems. For colloid systems, he finds the asymptotic probability density function displayed in Eq.(1.44) with a wavenumber-dependent mobility

$$F(q) = \frac{S(q)}{\rho} \sqrt{\frac{D_c^s(q)}{\pi}}, \quad (1.47)$$

which is valid for $q \ll a^{-1}$.

Kollmann's analysis predicts that the long-time behavior of quasi-one-dimensional diffusion is determined by the short-time *collective* dynamics of the system, which also incorporates the effect of hydrodynamic interactions. To understand this result, it should be realized that, owing to the absence of mutual particle passages in single-file diffusion, the motion of a density wave with $q \ll a^{-1}$ is reflected by the trajectory of every individual particle. In contrast, during normal (not single-file) diffusion, the motion of an arbitrarily chosen particle is completely decoupled from the collective motion of the system, and Eq.(1.46) does not apply.

1.2.1 Screened Hydrodynamic Interactions

When a particle moves through a fluid, it creates a flow that affects the velocities of other particles in its vicinity. Thus the motion of otherwise noninteracting Brownian particles can become correlated at times shorter than the collision time. For instance, during the diffusion of micro-size colloidal particles in a water-filled channel, it has been observed that several close-by particles exhibit a concerted motion by forming a dynamical "train" which lasts for a few seconds, signaling the existence

of hydrodynamic coupling [104].

Colloidal particles either in a finite container, near a single wall, or between two walls, have been studied. The hydrodynamic interactions in those geometries are always attractive (i.e., creating positive velocity correlations) and long-ranged: in an unbounded fluid, the interaction decays with interparticle distance r as $1/r$ [105]; the interaction between particles moving near and parallel to a single wall decays as $1/r^3$ [106, 107]; and for particle moving between and parallel to two walls, the interaction decays as $1/r^2$. More constrained geometries - perpendicular to the walls in a two-wall configuration and along a cylindrical channel - are essentially different, in that point disturbances should create flows with an exponential spatial decay [108, 109, 110].

To get a theoretical estimate of the hydrodynamic coupling, one needs in principle to calculate the Stokes flow due to the motion of two particles, subject to no-slip boundary conditions at the surface of the channel of radius R and particles of radius a . This is technically very difficult, and one thus has to resort to simplifying assumptions. It is thus assumed that the particle size is much smaller than both the channel width, $a \ll R$, and the interparticle distance, $a \ll r$. The latter requirement, though not strictly fulfilled in practice, allows one to treat the effect of one particle on the flow near the other one and near the walls, as if it were exerting a point force on the fluid. This is sometimes referred to as *Stokeslet approximation*. Therefore, to leading order in a/R or a/r , the flow induced by the motion of one particle in the vicinity of another is that of a point force. In addition, if we assume that the particle motion

is restricted to the central axis of the channel (which is reasonable in the case of colloidal suspensions), then the fundamental solution of the Stokes flow at the center of the channel is [104]

$$D_{12}(\xi) = (3/4)D_0 \frac{a}{R} \sum_{n=1}^{\infty} [a_n \cos(\beta_n \xi) + b_n \sin(\beta_n \xi)] e^{-\alpha_n \xi}. \quad (1.48)$$

In this equation, $\xi = z/R$, $u_n = \alpha_n + i\beta_n$ are respectively the complex roots of the equation, $u[J_0^2(u) + J_1(u)] = 2J_0(u)J_1(u)$, and $a_n + ib_n = 2/J_1^2(u_n) \{ \pi [2J_1(u_n)Y_0(u_n) - u_n(J_0(u_n)Y_0(u_n) + J_1(u_n)Y_1(u_n))] - u_n \}$ where J_ν and Y_ν are the Bessel functions of the first and second kind of order ν , respectively. For $\xi \ll 1$, the particles are insensitive to the walls, and the coupling approaches the algebraic $\sim 1/\xi$ dependence, like in an unbounded fluid. Yet, for $\xi \gg 1$, the confined geometry becomes manifest; the sum is dominated by its first term, and the interaction decays exponentially with distance (the coefficients of this term are $a_1 \simeq -0.037$, $b_1 \simeq 13.8$, $\alpha_1 \simeq 4.47$, and $\beta_1 \simeq 1.47$) [104].

In general, hydrodynamic interactions are long-ranged and are not pairwise additive. Screening of the hydrodynamic interaction between particles in a quasi-one-dimensional channel, on a length scale comparable with the channel diameter, implies that the concentration dependence of D_s^s is largely determined by *pair* hydrodynamic interactions [111].

1.2.2 Concentration Dependence of Self-Diffusion

Recently, Rice and coworkers [112] have calculated the influence of the hydrodynamic coupling between a colloid particle and the walls of a quasi-one-dimensional channel, and between pairs of colloid particles and the walls of the quasi-one-dimensional channel and each other, on the concentration dependence of the short-time single particle diffusion coefficient. Their approach is the following:

- (i) the hydrodynamic interaction is analyzed for the case of a fluid that can be described by the linear Navier-Stokes equations for incompressible stationary flow;
- (ii) an approximate solution for the concentration dependence of the single particle diffusion coefficient is obtained using the method of reflections, and an average is performed over all possible configurations of the particles.

According to their study, the two-particle diffusion tensor is given by

$$\begin{aligned} \frac{D_{11}(\xi)}{D_0} &= 1 + \chi_w + \chi_p(\xi) \\ &= 1 - \frac{1}{\pi} \int_0^\infty A d\alpha - \left[\frac{3\beta}{2\xi^2} - \frac{3\beta^3}{2\xi^4} - \frac{1}{\pi} \int_0^\infty B \alpha \sin(\alpha\xi) d\alpha \right] \times \\ &\quad \times \left[\frac{5\beta^3}{2\xi^2} - \frac{4\beta^5}{\xi^4} - \frac{2}{\pi} \int_0^\infty C \sin(\alpha\xi) d\alpha \right] \end{aligned} \quad (1.49)$$

$$\frac{D_{12}(\xi)}{D_0} = \frac{3\beta}{2\xi} - \frac{\beta^3}{\xi} - \frac{1}{\pi} \int_0^\infty A \cos(\alpha\xi) d\alpha + \chi_p(\xi), \quad (1.50)$$

with $\beta = a/R$. The function χ_w represents the effect of the wall, while the function $\chi_p(r)$ represents the effects of interactions between particles with separation r . The

other terms in Eq.(1.49) and Eq.(1.50) are

$$A = (\beta^3\alpha^2 + 3\beta)\frac{K_0(\alpha)}{I_0(\alpha)} - \frac{3\beta}{2I_0^2(\alpha)} + \frac{3\beta\alpha I_1^2(\alpha)}{2I_0^2(\alpha)} - \beta^3\alpha^2\frac{I_1(\alpha)}{I_0(\alpha)} + \frac{\beta^5\alpha^3}{6} \quad (1.51)$$

$$B = \left(\frac{\beta^3\alpha^2}{2} + 3\beta\right)\frac{K_0(\alpha)}{I_0(\alpha)} - \frac{3\beta}{2I_0^2(\alpha)} + \frac{\frac{3\beta\alpha I_1^2(\alpha)}{2I_0^2(\alpha)} - \frac{\beta^3\alpha^2 I_1(\alpha)}{2 I_0(\alpha)}}{\alpha I_1^2(\alpha) + 2I_0(\alpha)I_1(\alpha) - \alpha I_0^2(\alpha)} \quad (1.52)$$

$$C = \left(\frac{5}{2}\beta^3\alpha + \frac{2}{3}\beta^5\alpha^3\right)\frac{K_0(\alpha)}{I_0(\alpha)} - \frac{5\beta^3\alpha}{4I_0^2(\alpha)} + \frac{\frac{5\beta^3\alpha^2 I_1^2(\alpha)}{4I_0^2(\alpha)} - \frac{2\beta^5\alpha^3 I_1(\alpha)}{3 I_0(\alpha)} + \frac{\beta^7\alpha^4}{12}}{\alpha I_1^2(\alpha) + 2I_0(\alpha)I_1(\alpha) - \alpha I_0^2(\alpha)}, \quad (1.53)$$

where $I_\nu(\alpha)$ and $K_\nu(\alpha)$ are the modified Bessel functions of the first and second kind of order ν , respectively. It should be kept in mind that Eqs.(1.49) and (1.50) are far-field approximations. As the concentration is increased and the distance between particles becomes comparable to their size, the pair hydrodynamic interaction is affected by the presence of other particles. Then, a concentration-dependent correction factor, which involves the pair correlation function of the particles, is needed to account for the observed oscillations in $D_{11}(r)$ and $D_{12}(r)$ in concentrated dispersions.

When only pair hydrodynamic interactions are considered ⁴, Eq.(1.49) leads to the following result [112] for the short-time diffusion coefficient

$$\frac{D_s^s(\eta)}{D_0} = 1 + \chi_w + \frac{\eta}{\beta} \int_0^\infty d\xi g(\xi) \chi_p(\xi), \quad (1.54)$$

with $\eta = \rho\sigma = N\sigma/L$ the packing fraction of N particles of diameter $\sigma = 2a$ in

⁴It has been shown [111] that three-body contributions are small, even at high concentrations.

a channel of length L , and $g(r)$ is the pair distribution function. Since the colloid particles in this model system are constrained to move along the axis of the capillary, the assembly of colloid particles is equivalent to a one-dimensional fluid of hard rods for which the exact $g(r)$ is [113]

$$g(x) = \frac{1}{\eta} \sum_{k=1}^{\infty} \Theta(x-k) \left(\frac{\eta}{1-\eta} \right)^k \frac{(x-k)^{k-1}}{(k-1)!} \exp \left(-\frac{x-k}{\eta^{-1}-1} \right), \quad (1.55)$$

where $\Theta(x)$ is the unit step function and $x = r/\sigma$. Evaluation of the integral in Eq.(1.54) using the hard-rod pair distribution function for sterically stabilized colloids yields $D_s^s(\eta)/D_0$ as a function of η for given β . It is worth noting that $D_s^s(0)$ is smaller than what is predicted by the Stokes-Einstein relation for a particle in an infinite three-dimensional liquid, due to the effects of the nearby channel walls. When a particle is close to a wall, it is customary to represent the effect of that wall on $D_s^s(0)$ by the multiplicative factor Λ^{-1} , i.e., $D_s^s(0) = D_0/\Lambda$, which in terms of the former result yields $\Lambda = (1 + \chi_w)^{-1}$ [114, 37].

Chapter 2

Diffusion of Colloids in Confined Colloid-Polymer Mixtures

A detailed description is given of the model used to study the diffusion of colloids in a colloid-polymer mixture confined in a channel. First, the binary mixture is mapped into an effective one-component system of colloids in one dimension and then methods from the theory of diffusion together with Monte Carlo simulations are employed to study the diffusion dynamics of colloids in the mixture.

2.1 Mapping to Effective One-Component System

When non-adsorbing polymers are added to a suspension of hard sphere-like colloidal particles, an effective, generally attractive interaction is induced between the colloidal particles. The origin of this interaction is the so-called depletion effect: the exclusion

of polymer from the depletion zone between nearby colloids gives rise to an unbalanced osmotic pressure. Alternatively, one can view the depletion induced attraction as arising from an increase in the entropy of the polymers: when two colloids approach each other closely, their depletion zones start to overlap and offer the polymer more free volume to explore, thereby yielding a gain in entropy. Asakura and Oosawa [115], using an idealized picture, showed that the range of the depletion interaction is determined by the diameter of the polymer coils, and its strength is proportional to the activity of the polymer reservoir.

In order to develop the statistical mechanics of such mixtures, it is necessary to specify a suitable model Hamiltonian. This was first done by Vrij [116], who considered a zeroth-order model in which the colloid-colloid interaction is hard sphere-like, with colloids of diameter σ_c , and with polymers taken as ideal interpenetrating coils, as Asakura and Oosawa had assumed. However, polymers are excluded by a center-of-mass distance $(\sigma_c + \sigma_p)/2$ from the colloids. The solvent is treated as an inert continuum. It is found [117, 118, 119] that for size ratios $\sigma_p/\sigma_c \equiv q < 2/\sqrt{3} - 1 \cong 0.1547$, this binary mixture in two and three dimensions can be mapped exactly onto an effective one-component Hamiltonian for the colloids which contains only zero, one and two-body (pairwise) contributions.

We turn next to the case of one dimension. Omitting trivial kinetic energy terms, the Hamiltonian is given by the $H = H_{cc} + H_{cp} + H_{pp}$, where H_{cc} denotes the colloid-colloid Hamiltonian, H_{cp} the colloid-polymer Hamiltonian, and H_{pp} the polymer-

polymer Hamiltonian,

$$\begin{aligned}
 H_{cc} &= \sum_{i < j}^{N_c} \phi_{cc}(X_{ij}) \\
 H_{cp} &= \sum_{i=1}^{N_c} \sum_{j=1}^{N_p} \phi_{cp}(X_i - x_j) \\
 H_{pp} &= \sum_{i < j}^{N_p} \phi_{pp}(x_{ij}) = 0,
 \end{aligned} \tag{2.1}$$

where X_i denotes the center of colloid i , x_i that of polymer i , $X_{ij} = |X_i - X_j|$, and $x_{ij} = |x_i - x_j|$. The pair potentials are given by

$$\begin{aligned}
 \phi_{cc}(X_{ij}) &= \begin{cases} \infty & \text{for } X_{ij} < b \\ 0 & \text{otherwise} \end{cases} \\
 \phi_{cp}(X_i - x_j) &= \begin{cases} \infty & \text{for } |X_i - x_j| < (a + b)/2 \\ 0 & \text{otherwise} \end{cases} \\
 \phi_{pp}(x_{ij}) &= 0,
 \end{aligned} \tag{2.2}$$

where a and b denote the length of the polymer and colloid rods, respectively.

As always, the quantity which needs to be evaluated is the partition function. For systems with purely hard interactions, this is equal to the ‘volume’ available on the line. However, in the case of the Asakura-Oosawa model, this available volume depends upon the way in which the two different species are ordered in each configuration. For the general case of N_c colloidal rods and N_p ideal polymer rods, the calculation clearly presents a difficult combinatorial problem. As Evans et al. [118] have shown, this difficulty can be bypassed by integrating out the polymer degrees of

freedom, leading to an effective Hamiltonian for the colloids. Unlike the case of three and two dimensions, truncation of the series of cluster integrals after the two-body interaction terms is exact for $q \equiv a/b < 1$. Nevertheless, it is not entirely clear how a physical interpretation can be given to the one-dimensional pair ‘depletion’ potential; there is indeed no longer an intuitive picture of the polymer being excluded from the region between the colloids. The effective pair potential must now be regarded as one of combinatorial origin, which simply reflects the fact that more weight is given to particular configurations of the colloids as a result of the number of ways in which the polymer can be positioned around them. The same interpretation appears to be called for in the study by Widom and Lekkerkerker [120].

In order to integrate out the polymer degrees of freedom, consider a homogeneous mixture in the semi-grand canonical (N_c, L, z_p, T) ensemble, and write the corresponding thermodynamic potential F in one-component form

$$\exp(-F/k_B T) = \frac{1}{N_c! \Lambda_c^{N_c}} \int dX_1 \dots \int dX_{N_c} \exp[-(H_{cc} + \Omega)/k_B T], \quad (2.3)$$

where $z_p = \Lambda_p^{-1} \exp(\mu_p/k_B T)$ is the activity of the polymer reservoir and Λ_ν is the thermal de Broglie wavelength of species ν , with $\nu = c, p$. The grand potential of the ideal polymer coils in the external field of a fixed configuration of N_c colloids with coordinates $\{X_i\}$, with $i = 1, 2, \dots, N_c$ can be expanded in terms of the colloid-polymer Mayer f -function $f_{ij} \equiv f(X_i, x_j) = \exp[-\phi_{cp}(X_i - x_j)/k_B T] - 1$,

$$-\frac{\Omega}{k_B T} = z_p \int dx_j + \sum_{i=1}^{N_c} z_p \int dx_j f_{ij} + \sum_{i < k}^{N_c} z_p \int dx_j f_{ij} f_{kj} + \dots \quad (2.4)$$

The expansion can be written as a sum of contributions Ω_n , which are classified according to the number $n = 0, 1, 2, \dots, N_c$ of colloids which interact simultaneously with the ‘sea’ of ideal polymers, i.e.,

$$\begin{aligned} \Omega &= \Omega_0 + \Omega_1 + \Omega_2 + \dots \\ &= -z_p L k_B T + z_p N_c (a + b) k_B T + \sum_{i < j}^{N_c} \phi(X_{ij}) + \dots \end{aligned} \quad (2.5)$$

The zero and one-body terms are independent of the colloidal coordinates and have the following interpretations: Ω_0 is the grand potential of ideal polymer rods in a length L at activity z_p , since $z_p = P_p^r / k_B T = \rho_p^r$, where P_p^r is the pressure and ρ_p^r the number density of the ideal polymer in the reservoir, and Ω_1 / N_c is the grand potential required to insert a single colloid in the sea of ideal polymer. The third term is the sum of pair potentials, with the effective pair potential $\phi(X)$ given by a simple linear function

$$\phi(X) = \begin{cases} 0 & |X| > (a + b) \\ -z_p k_B T (a + b - |X|) & b < |X| < (a + b) \end{cases}; \quad (2.6)$$

$\phi(X)$ is the one-dimensional Asakura-Oosawa depletion potential; $(a + b - |X|)$ is simply the difference in accessible length for the polymers when the colloids are separated by a distance $|X|$ and when their separation is infinite. The higher-order terms in Eq.(2.5) correspond to three-body, four-body, etc., potentials. In general, the expansion contains N_c terms. However, it is easy to show that provided that $q < 1$, three- and higher-body potentials are identically zero. This follows from the fact that a smaller polymer cannot simultaneously overlap with three non-overlapping colloids.

Thus, for $q < 1$ the effective one-component Hamiltonian for the colloids reduces to the simple form [121]

$$\begin{aligned} H_{eff} &= H_{cc} + \Omega \\ &= \Omega_0 + \Omega_1 + \sum_{i < j} \phi_{eff}(X_{ij}), \end{aligned} \quad (2.7)$$

where the effective pair potential

$$\phi_{eff}(X) = \phi_{cc}(X) + \phi(X) \quad (2.8)$$

consists of a hard core with an attractive linear portion whose (finite) range is equal to a , the length of a polymer rod, and whose value at contact is $z_p k_B T a$. In this exact mapping, the complex binary mixture problem has been reduced to that of a one-component fluid in one dimension for which the particles interact via the nearest-neighbor pair potential ϕ_{eff} . The free energy and equation of state of such a fluid can be determined exactly and analytically by utilizing standard Laplace transform techniques [113].

At this point, we have to find a relation between the packing fraction of polymer in the system and the packing fraction of polymer in the reservoir. Introducing $\gamma(z_p, \eta_c) = \langle N_p \rangle_{z_p} / L \rho_p^r$ as the ratio of the density of polymer in the mixture to that in the reservoir, the packing fraction of polymer in the system can be written as $\eta_p = \gamma \eta_p^r$. Using the following identity for the thermodynamic potential of a binary mixture

$$F(N_c, L, z_p) = F(N_c, L, z_p = 0) - k_B T L \int_0^{z_p} dz'_p \gamma(z'_p, \eta_c), \quad (2.9)$$

the free volume fraction γ is obtained from

$$\gamma(z_p, \eta_c) = - \left(\frac{\partial F(N_c, L, z_p)/k_B T}{L \partial z_p} \right)_{N_c, L}. \quad (2.10)$$

In these equations, η_p and η_p^r are the packing fractions of polymer in the system and in the reservoir, respectively, and η_c is the colloid packing fraction.

2.2 Self-Diffusion and Mobility of Colloids

Consider a mixture of colloids and polymers in a solvent confined in a cylindrical channel (Fig.2.1). In the Asakura-Oosawa model, colloid-colloid and colloid-polymer interactions are just hard-core repulsions, whereas polymers do not interact with each other at all. Furthermore, colloids cannot pass each other if the channel is narrow enough, so that their motion will effectively be restricted to translations along the central axis of the channel. On the other hand, depending on its size, the polymer can be regarded in limiting cases as a one-dimensional rod of length $2R_g$ or as a three-dimensional sphere of radius R_g .

In the first case, as mentioned above, the binary mixture can be reduced (at least from the thermodynamics point of view) to an effective one-component system with a modified Hamiltonian, and this reduction is exact for $q < 1$. In the second case, the situation is different, in the sense that we have to use a modified depletion potential for colloid-polymer mixtures interacting in the bulk, due to the presence of the walls. Neglecting three- and higher-body potentials, the effective Hamiltonian for a mixture



Figure 2.1: Schematic representation of a confined colloid-polymer mixture in the single-file regime of the colloids.

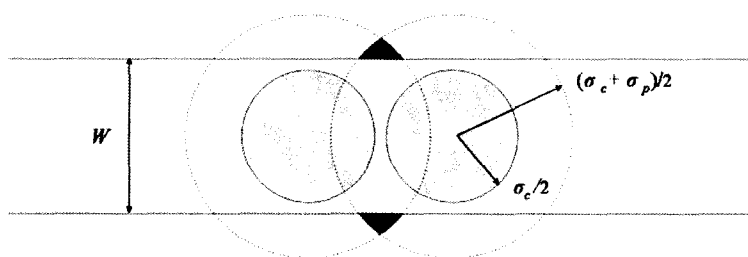


Figure 2.2: Schematic representation of the depletion zone of polymers in a channel (overlapping portion of the two dotted circles). The blue circles are colloids and the red-filled region is that part of the depletion zone taken up by the walls.

in the bulk may be written as

$$H_{eff} = H_0 + \sum_{i < j}^{N_c} \phi_{eff}(R_{ij}), \quad (2.11)$$

with effective pair potential

$$\phi_{eff}(R_{ij}) = \phi_{cc}(R_{ij}) + \phi_{AO}(R_{ij}), \quad (2.12)$$

and

$$H_0 = \Omega_0 + \Omega_1 = -z_p k_B T [1 - \eta_c (1 + q)^3] V, \quad (2.13)$$

where $\{R_i\}$ denotes the position coordinates of colloids and ϕ_{AO} is the pair potential of Asakura-Oosawa [122], which describes an attractive potential well close to the surface of the colloid, and is given by

$$\phi_{AO}(R_{ij}) = \begin{cases} -\frac{\pi}{6} \sigma_p^3 \left(\frac{1+q}{q}\right)^3 z_p k_B T \times \\ \quad \times \left[1 - \frac{3R_{ij}}{2(1+q)\sigma_c} + \frac{R_{ij}^3}{2(1+q)^3 \sigma_c^3} \right] & \sigma_c < R_{ij} < \sigma_c + \sigma_p \\ 0 & R_{ij} > \sigma_c + \sigma_p. \end{cases} \quad (2.14)$$

Although the geometry in three dimensions is less forgiving than that in one dimension, and the mapping to an effective one-component is only exact for $q < 0.1547$, this result is valid for our quasi one-dimensional model up to $q = 1$ because, as noted above, a smaller polymer cannot simultaneously overlap with three non-overlapping colloids. Meanwhile, the sum in Eq.(2.11) reduces to a sum only over immediate neighboring colloids.

If we take into account the fact that the Asakura-Oosawa potential is actually proportional to the difference in free volume of the polymers between the case where two colloids are separated by a finite distance $R_{ij} = |\mathbf{R}_i - \mathbf{R}_j|$ and the case where they are separated by an infinite distance, then it becomes clear that we should subtract the volume of that part of the depletion zone which has been taken by the walls from the total overlap volume. In practice this volume is negligible, unless the walls are very close to the surface of the colloids or the size ratio is not far from unity (see Fig. 2.2). For a *rectangular* channel of width w , which is often used in actual diffusion experiments, and for $w^2 > (1 + q)^2 \sigma_c^2 - r^2$, which is usually satisfied, this volume is found to be

$$\frac{\Delta V}{\frac{\pi}{6} \sigma_p^3} = 4 \int_{\delta}^{\sqrt{1-r^2}/2} dy \left(\int_0^{\sqrt{(1-r^2)/4-y^2}} dx [-r + \sqrt{1 - 4(x^2 + y^2)}] \right), \quad (2.15)$$

where r is the distance between two adjacent colloids and δ is the distance between the walls and the center line of the channel, both reduced by $\sigma_c + \sigma_p$.

We could successfully map the binary mixture to an effective one-component system as far as direct interactions are concerned. However, when it comes to hydrodynamic interactions, reduction of the mixture by integrating out polymer degrees of freedom is a very difficult task, if possible at all, especially since hydrodynamic interactions are not pairwise-additive in general. But we may think of polymers in solution as an effective medium with a modified viscosity which depends on the polymer concentration. This means that we only consider the impact of the polymer on the hydrodynamic motion of colloids through a change of the diffusivity of a free colloid

from D_0 to $D_0(\zeta_0/\zeta_{eff})$, where ζ_{eff} is the effective friction coefficient corresponding to the modified viscosity. This approximation enables us to obtain an explicit expression for the concentration dependence (η_c and η_p) of the self-diffusion coefficient⁵ and mobility factor of the colloids in a colloid-polymer mixture.

In order to find the self-diffusion and mobility from equilibrium ensemble averages, we need to know the two-point equilibrium distribution functions $g(r)$ analytically without approximation. The model described above is in essence a one-dimensional model with nearest-neighbor interactions. For these types of systems, there is a systematic analytic method to calculate $g(r)$ exactly. Unfortunately, for models in the continuum such as the present one, the result can only be given as an infinite series which involves increasingly complicated inverse Laplace transforms. In particular, for finite-range isotropic pair potentials which have a hard core of diameter (length) σ , $g(r)$ is given by [123]

$$\begin{aligned} g(r = |R - R'|) &= \frac{1}{\rho^2} \left\langle \sum_{k=1}^N \sum_{j=1 \neq k}^N \delta(R_k - R) \delta(R_j - R') \right\rangle \\ &= \frac{1}{\rho} \sum_{k=1}^{\infty} \Theta(r - k\sigma) \frac{1}{2\pi i} \int_{c-i\infty}^{c+i\infty} ds e^{r(s-c)} \left(\frac{\tilde{J}(s)}{\tilde{J}(c)} \right)^k, \end{aligned} \quad (2.16)$$

where $c = p/k_B T$, Θ is the Heaviside step function, and \tilde{J} is the Laplace transform of the Boltzmann factor for the pair potential $\phi(r)$, i.e.,

$$\tilde{J}(s) = \mathcal{L}\{e^{-\phi(r)/k_B T}\} = \int_0^{\infty} dr \exp(-sr - \phi(r)/k_B T). \quad (2.17)$$

⁵In the case of mixtures, the term tracer-diffusion is sometimes used instead of self-diffusion.

The pressure p in the system at a fixed bulk density is given by

$$\rho = -\frac{\tilde{J}(p/k_B T)}{\tilde{J}'(p/k_B T)}. \quad (2.18)$$

Analytic closed-form evaluation of the sum in Eq.(2.16), even for the linear potential of Eq.(2.6) is feasible for short separations [124], but is otherwise tedious and must practically be performed numerically. An alternate way to get accurate results for $g(r)$ is through Monte Carlo simulations, which then can be used to compute D_s^s from Eq.(1.54).

As mentioned earlier, for non-passing colloids the long-time diffusion coefficient is zero because of the anomalous diffusion stemming from the single-file motion of particles. In this case, the proportionality factor relating the mean-squared displacement of the tagged particle to the square root of time is called the mobility factor, which can be related to the short-time collective dynamics of the system. It is seen from Eq.(1.35) that finding D_c^s requires obtaining the static structure factor $S(k)$, which is directly related to the Fourier transform of $g(r)$

$$S(k) = \frac{1}{N} \langle \delta n(\mathbf{k}) \delta n(-\mathbf{k}) \rangle = 1 + \rho \int e^{i\mathbf{k}\cdot\mathbf{r}} g(r) d\mathbf{r}, \quad (2.19)$$

where $\rho = N_c/V$ is the number density of colloids. In the case of a one-dimensional geometry, the above equation leads to

$$S(k) = 1 + 2\rho \operatorname{Re} \int_0^\infty e^{ikx} g(x) dx, \quad (2.20)$$

with $\rho = N_c/L$.

The hydrodynamic function defined in Eq.(1.36) can be further simplified and made more explicit. The “diagonal” terms ($i = j$) in the double sum yield precisely the expression for the short-time self-diffusion coefficient. At the pair level, we can use the two-body microscopic diffusion tensor given by Eq.(1.50). Each of the remaining “off-diagonal” terms ($i \neq j$) contributes equally, so that the sum may be replaced by an ensemble average of just one pair of particles (for example $i = 1$ and $j = 2$), multiplied by twice the number of pairs, i.e., $N(N - 1) \approx N^2$. We thus get

$$H(k) = \frac{1}{D_0} \left(D_s^s + \rho \int_0^\infty dx D_{12}(x) g(x) \cos(kx) \right). \quad (2.21)$$

2.3 Results and Discussion

The short-time self-diffusion coefficient of colloids in a colloid-polymer mixture has been computed and compared with the short-time self-diffusion coefficient of colloids in a pure colloidal dispersion. The diagonal elements of the two-body microscopic diffusion tensor are given by a modified version of Eq.(1.49), which incorporates concentration corrections [112]. The short-time self-diffusion coefficient is obtained by taking the equilibrium ensemble average of these elements. An essential ingredient of this calculation is the colloidal pair distribution function, which is obtained from the Monte Carlo simulations. The computer code was first validated by reproducing the correct distribution function $g(r)$ in three-dimensions [118]. Fig.2.3 shows $g(r)$ for two selected values of η_c . Comparing with the pair distribution function of pure

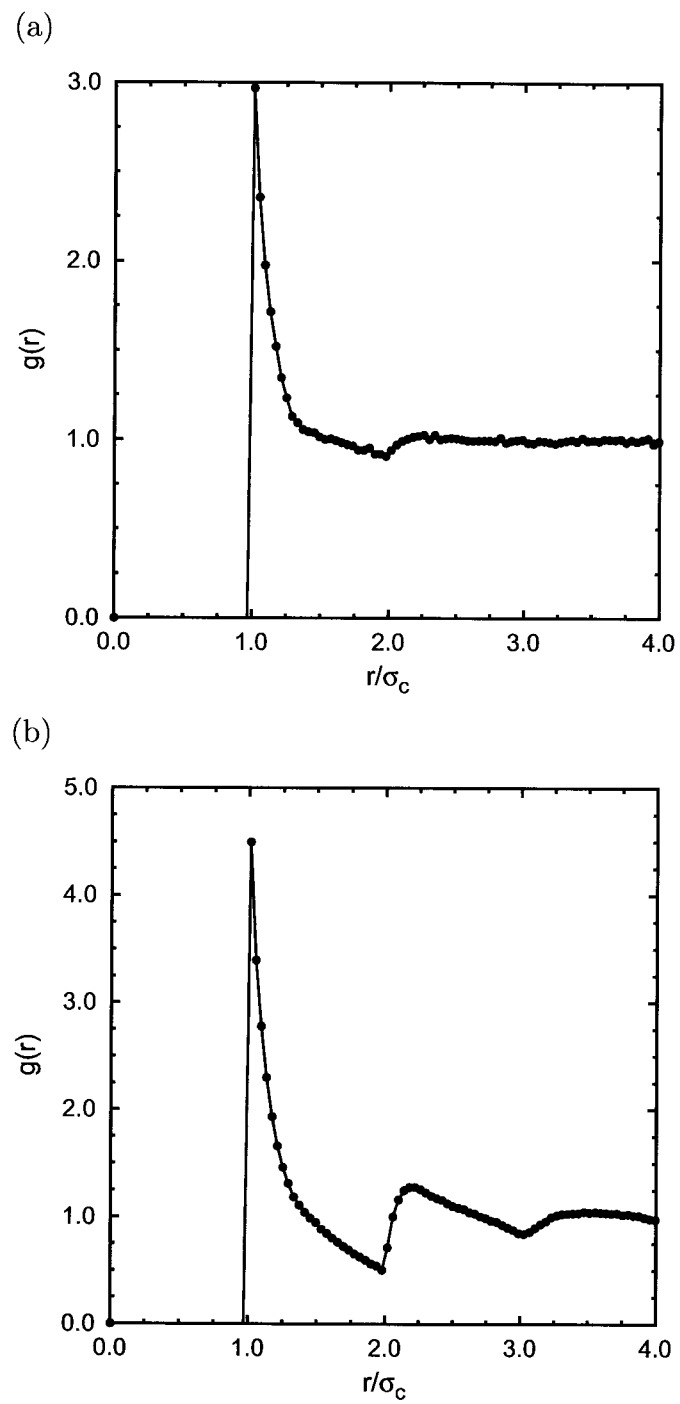


Figure 2.3: Radial distribution function of colloids in a confined colloid-polymer mixture at $\eta_p = 0.2$ and $q = \sigma_p/\sigma_c = 0.4$; (a) $\eta_c = 0.2$. (b) $\eta_c = 0.6$.

colloids ⁶ reveals that the depletion interaction leads to a higher value of $g(\sigma_c)$, as expected.

The reduction of the self-diffusion coefficient of colloids upon addition of polymers to the solution is depicted in Fig.2.4. It is customary to write the diffusion coefficient in terms of a virial expansion in density or volume fraction. The second virial coefficient is negative in our case, in contrast to the case of diffusion of colloids in bulk solutions. Next, the short-time collective diffusion coefficient and long-time mobility of colloids in a colloid-polymer mixture are determined. The off-diagonal elements of the microscopic diffusion tensor appear in the hydrodynamic function $H(q)$, and are given by Eq.(1.50). As is already seen, the calculation of $D_c^s(q)$ and $F(q)$ requires the knowledge of the colloid-colloid pair distribution function as well as of the static structure factor of colloids in the presence of polymers. The structure factor of colloids in a colloid-polymer mixture attains a higher value at zero wavenumber (long wavelength), and its first peak shifts towards shorter wavelengths (see Fig.2.5).

The variation of D_{12} with separation in a concentrated solution is illustrated in Fig.2.6. The red curve contains the correction required at high concentrations, while the green curve neglects this effect. However, eventually, there is only a slight difference between the acquired D_c^s . Fig.2.7 exhibits an interesting feature of D_c^s , short-time gradient diffusion coefficient, namely, its growth with concentration, which distinguishes it from the short-time self-diffusion. This behavior is the result of the rapid

⁶The contact value of $g(r)$ is $(1 - \eta_c)^{-1}$ for a one-dimensional hard-rod fluid.

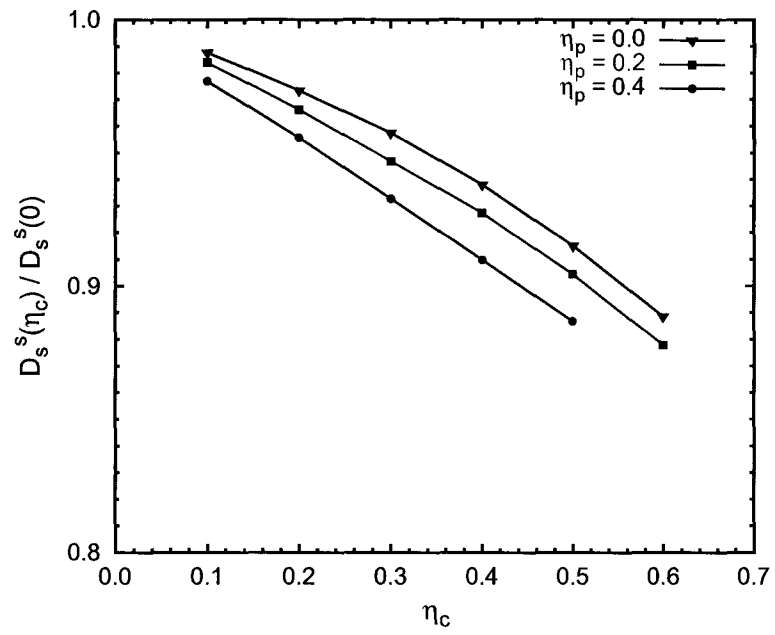


Figure 2.4: Short-time self-diffusion coefficient of colloids in solution with and without the presence of polymer depletion. $\beta = a/R = 0.216$ and $q = 0.4$.

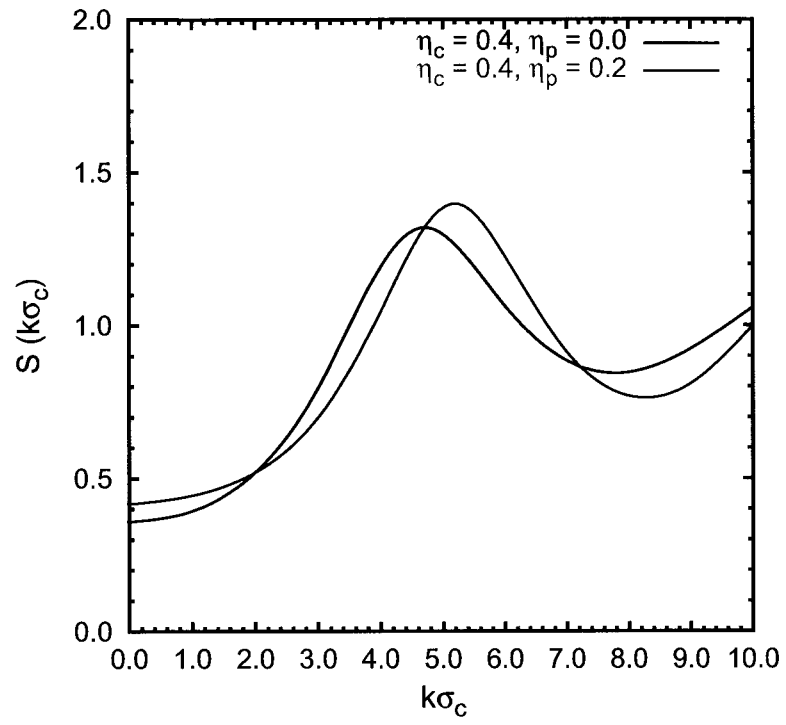


Figure 2.5: Static structure factor of colloids with and without the presence of polymer ($q = 0.4$).

relaxation of inhomogeneities at high colloid concentrations. It also shows that the addition of polymer reduces the gradient diffusion of colloids, in accord with intuition. In contrast to the gradient diffusion coefficient, the long-time mobility factor is enhanced in systems with short-range attractive interactions in one dimension compared to systems where hard-core repulsive forces are the only source of direct interactions (Fig.2.8). This is in agreement with the picture given in [125], in which the drag force on a colloid inside the depletion layer is merely exerted by the solvent, whereas outside the depletion layer, the drag force is exerted by the polymer solution. Thus, the outcome is a friction coefficient less than what is obtained in a system with no depletion effect.

Our predictions are in qualitative agreement with the experimental results that have been performed previously in our group [126]. The reduction of the self-diffusion coefficient given by the slope of the curves in Fig.2.9 at short times, is evident. Unfortunately, quantitative agreement cannot be verified, since the theory developed here gives the normalized diffusion coefficients and mobility of colloids in the mixture. The normalization factor is the diffusion coefficient or mobility of colloids at infinite dilution ($\eta_c = 0$) and at a given polymer packing fraction (η_p), and thus is inversely proportional to the friction exerted on a single colloid slowly dragged in a polymer solution. Moreover, additional experimental data, in particular for the long-time limit, would be useful.

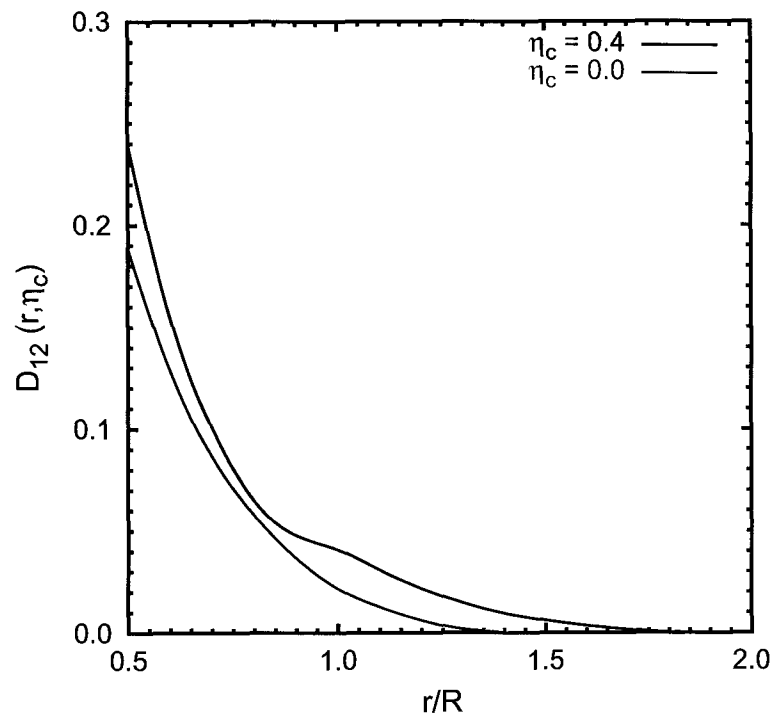


Figure 2.6: Comparison of the expressions for D_{12} ; the red curve represents the one which incorporates the concentration dependence, while the green curve represents the one with no such correction (infinite dilution). In both cases $\beta = 0.216$.

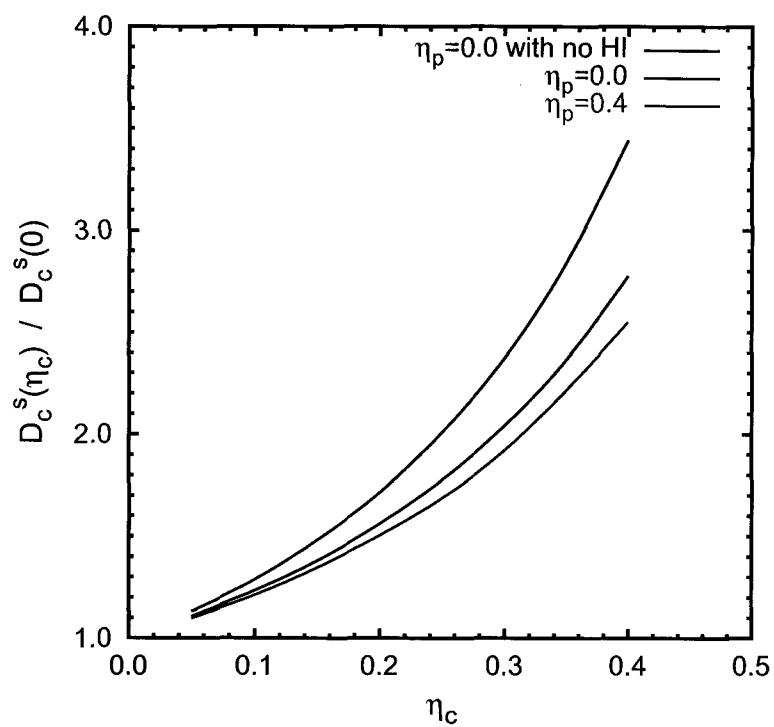


Figure 2.7: Short-time gradient diffusion coefficient of colloids in solution with and without polymer. The case where hydrodynamic interactions (HI) are absent is also plotted for reference. $\beta = a/R = 0.216$ and $q = 0.4$.

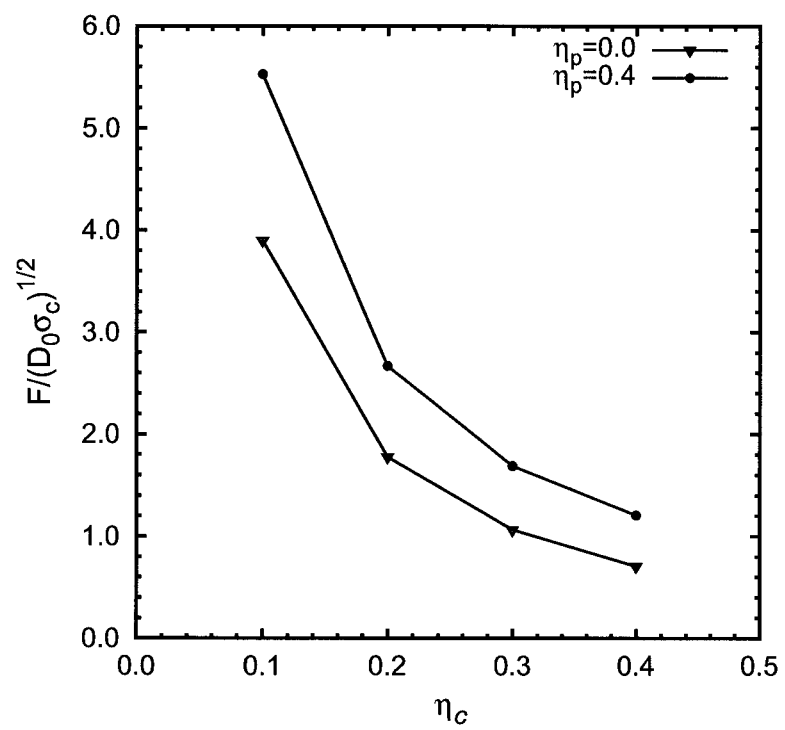


Figure 2.8: Long-time mobility factor of colloids in solutions with and without polymer. $\beta = a/R = 0.216$ and $q = 0.4$.

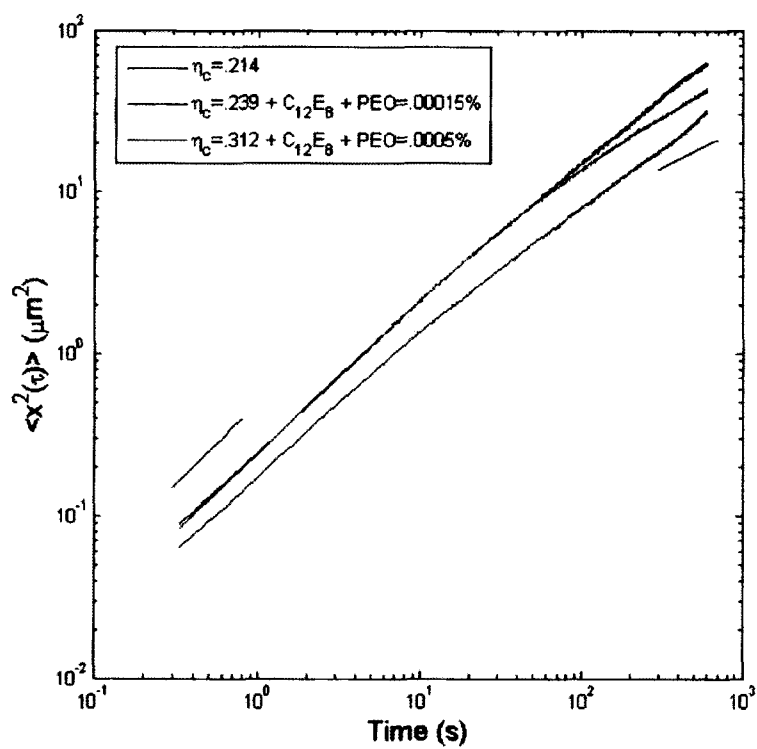


Figure 2.9: Mean-squared displacement of colloids in a channel for various polymer concentrations (adapted from [126]).

Chapter 3

Diffusion of a Polymer in Confined Colloid-Polymer Mixtures

In this chapter, we describe the dynamics of a single polymer chain in a colloidal suspension confined in a narrow channel. The colloids are modeled as hard obstacles and the polymer is modeled as a Gaussian or self-avoiding chain depending on the quality of the solvent.

3.1 General Formalism

The method described in the previous chapter does not take into account the internal degrees of freedom and the structure of the polymer. More importantly, it cannot provide any information on the dynamics of the polymers.

The theoretical foundation of the current understanding of transport properties

of macromolecules in bulk dilute solutions may be traced back to the pioneering works of Kirkwood [127] and Zimm [128], who elucidated the importance of the hydrodynamic interactions in the dynamic properties of macromolecules in solution. Subsequent developments by Fixman [129, 130] provided a general framework for polymer dynamics that accounted for excluded-volume effects and chain stiffness. As a result, calculated transport properties of macromolecules can now be quantitatively compared with measurements.

Due to the success of the Kirkwood formalism for computing transport coefficients in bulk solutions, this approach will be employed here. Such an approach yields approximate expressions for diffusion coefficients, including numerical prefactors. We will focus on the case of flexible linear polymers in a cylindrical capillary, first in the absence of colloids, and then in the presence of colloids.

Consider a single polymer consisting of N monomeric units suspended in a quiescent incompressible Newtonian solvent of viscosity η_s . We will view the monomers as spherical Brownian particles of radius b and friction constant $\zeta = 6\pi\eta_s b$, and the link between neighboring monomers as permanent but flexible bonds maintained by some internal potential between them. In addition, there may also be a long-range interaction between non-bonded monomers, e.g., the excluded volume interaction. We will lump all internal interactions into one potential, U_{int} . In general, if an external force \mathbf{F}_j is applied to each monomer j and no external torques are applied, the induced

velocity of, say, monomer i , in the overdamped limit, has the following form

$$\mathbf{v}_i = \sum_{j=1}^N \mathbf{H}_{ij} \cdot \mathbf{F}_j, \quad (3.1)$$

which defines the matrix of mobility tensors \mathbf{H}_{ij} ⁷.

One can obtain an expression for \mathbf{H}_{ij} by solving the creeping flow equations of low-Reynolds number hydrodynamics subject to appropriate boundary conditions. For our present purposes, we assume the confining capillary of radius R to be oriented in the z -direction. Hence, we need only the zz component of \mathbf{H} , which in the Stokeslet approximation (point force) is given by [131]

$$H_{zz}(\mathbf{r}, \mathbf{r}') = \int_{-\infty}^{+\infty} \frac{dk_{\parallel}}{2\pi} \sum_{n=-\infty}^{\infty} \sum_{m=1}^{\infty} (1 - \hat{k}_z \hat{k}'_z) \frac{J_n(\alpha_{nm}\rho/R) J_n(\alpha_{nm}\rho'/R)}{\pi \eta_s (kR)^2 J_{n+1}^2(\alpha_{nm})} e^{in(\phi-\phi')} e^{ik_{\parallel}(z-z')}, \quad (3.2)$$

where $k^2 = k_{\parallel}^2 + (\alpha_{nm}/R)^2$, \hat{k} is a unit vector in the \mathbf{k} direction, k_{\parallel} is the z component of \mathbf{k} , $J_n(x)$ is the Bessel function of the first kind of order n and α_{nm} is its m^{th} zero, and where we use cylindrical coordinates, $\mathbf{r} \equiv (\rho, \phi, z)$. Notice that H_{zz} is not a function of $\mathbf{r} - \mathbf{r}'$ in confined geometries, due to the broken translational symmetry. Note also that H_{zz} diverges at $\mathbf{r} = \mathbf{r}'$. Hence a short-range cutoff is implicit in Eq.(3.2).

To determine the matrix of mobility tensors \mathbf{H}_{ij} for the confined Brownian particles, we note that the no-slip (stick) boundary conditions between the particles and the solvent imply that particles move with the local solvent velocity, that is, $H_{ijzz} = H_{zz}(\mathbf{r}_i, \mathbf{r}_j)$. Having obtained the mobility matrix for a collection of Brownian

⁷The relation between \mathbf{H}_{ij} and \mathbf{D}_{ij} (defined in Section 1.1.3) is simply: $\mathbf{D}_{ij} = k_B T \mathbf{H}_{ij}$.

particles in a cylinder, we can now calculate the Kirkwood estimate for the diffusion constant D_{\parallel} for the center-of-mass motion along the axis of symmetry of the cylindrical capillary.

Several computational schemes are possible. We will use a Langevin equation for the motion of the particles. Consider a weak, constant force field F_z in the z -direction applied to the center of mass of the collection of Brownian particles (i.e., a force *per particle* F_z/N). This applied field will induce the center of mass to move with some steady-state velocity $\langle v_{cm} \rangle$. The ratio of this induced velocity to the applied force is the total mobility of the macromolecule, μ_{tot} . The diffusion constant D_{\parallel} is related to μ_{tot} via the fluctuation-dissipation theorem, $D_{\parallel} = k_B T \mu_{tot}$, i.e.,

$$D_{\parallel} = k_B T \langle v_{cm} \rangle / F . \quad (3.3)$$

The motion of a single monomer in the z -direction obeys

$$v_i = \sum_{j=1}^N H_{ijzz} \left(-\frac{\partial U_{int}}{\partial z_j} + F_z/N + f_j(t) \right) , \quad (3.4)$$

where z_j is the z coordinate of monomer j , U_{int} is the internal contribution to the particle potential, and $f_j(t)$ is a random Brownian force in the z -direction originating from collisions between solvent molecules and monomer j . The distribution of $f_j(t)$ is assumed to be Gaussian, and characterized by its moments: $\langle f_j(t) \rangle = 0$ and $\langle f_j(t) f_j(t') \rangle = 2H_{ijzz}^{-1} k_B T \delta(t - t')$. Summing Eq.(3.4) over i and dividing by N gives an equation for the center-of-mass velocity in the z -direction

$$v_{cm} = \frac{1}{N} \sum_{i=1}^N \sum_{j=1}^N H_{ijzz} (F_z/N + f_j(t)) . \quad (3.5)$$

Note that in the double sum over all particles, the contributions from the interparticle potential cancel as a result of the action-reaction principle. Thermal averaging of Eq.(3.5) and using Eq.(3.3) then yields the diffusion constant.

Performing this average, however, is not feasible in general due to the complicated structure of the mobility matrix \mathbf{H}_{ij} . To simplify the analysis, a preaveraging approximation is traditionally employed in which the thermal average of the terms in Eq.(3.3) is broken into the products of the equilibrium averages of the forces and of the H_{ijzz} . This amounts to replacing H_{ijzz} by

$$\langle H_{ijzz} \rangle_{\text{eq}} = \int D(\{\mathbf{R}_n\}) H_{ijzz} \Psi_{\text{eq}}(\{\mathbf{R}_n\}) \quad (3.6)$$

in Eq.(3.5) prior to thermal averaging, where Ψ_{eq} is the equilibrium distribution function of the macromolecule, and $D(\{\mathbf{R}_n\})$ indicates that a *functional* integration over all particle configurations is to be carried out. The resulting expression for D_{\parallel} is given by

$$D_{\parallel} = \frac{k_B T}{N^2} \sum_{i=1}^N \sum_{j=1}^N \langle H_{ijzz} \rangle_{\text{eq}}. \quad (3.7)$$

The main difficulty encountered in using the formalism described above to compute D_{\parallel} for a particular polymer system lies in the computation of the equilibrium averages. Such averages require knowledge of the two-point distribution function $\Psi_{\text{eq}}(\mathbf{r}_i, \mathbf{r}_j)$ for a polymer in a confined geometry. Unfortunately, even the two-point distribution function for an unconfined self-avoiding polymer is unknown. In such cases, one must resort to scaling theories or to various approximate self-consistent calculations. And even when $\Psi_{\text{eq}}(\mathbf{r}_i, \mathbf{r}_j)$ is known, computation of these averages for

arbitrary capillary sizes can be quite tedious. This analysis may, however, be substantially simplified by considering the limit of very narrow capillaries, i.e., of radius much smaller than the mean size of an unconfined polymer. This happens to be also the case of most technological interest.

3.2 Polymer in a Θ Solvent -

The Gaussian Model

First, let us rewrite the expression for D_{\parallel} given by Eq.(3.7) in the more compact form

$$D_{\parallel} = \frac{k_B T}{N^2} \int_{-\infty}^{+\infty} \frac{dk_{\parallel}}{2\pi} \sum_{i,j=1}^N \sum_{n=-\infty}^{\infty} \sum_{m=1}^{\infty} \mathbf{P}(\mathbf{k})_{zz} \frac{\langle \mathcal{H}(i, j; n, m, k_{\parallel}) \rangle_{\text{eq}}}{\pi \eta_s (kR)^2 J_{n+1}^2(\alpha_{nm})}, \quad (3.8)$$

where $\mathbf{P}(\mathbf{k})_{zz} = 1 - \hat{k}_z \hat{k}_z$ and where the kernel $\langle \mathcal{H}(i, j; n, m, k_{\parallel}) \rangle_{\text{eq}}$ is given by

$$\langle \mathcal{H}(i, j; n, m, k_{\parallel}) \rangle_{\text{eq}} \equiv \langle J_n(\alpha_{nm} \rho_i / R) J_n(\alpha_{nm} \rho_j / R) \exp[in(\phi_i - \phi_j)] \exp[ik(z_i - z_j)] \rangle_{\text{eq}}. \quad (3.9)$$

For the Gaussian chain model of polymer chains in a Θ solvent, the exact two-point distribution function may be obtained for arbitrary capillary size [40]. Furthermore, the two-point distribution function may be factored into the product of a longitudinal and a transverse distribution function $\Psi_{\text{eq}}(\mathbf{r}_i, \mathbf{r}_j) = \psi_{\parallel}(z_i - z_j; |i - j|) \psi_{\perp}(\boldsymbol{\rho}_i, \boldsymbol{\rho}_j; i, j)$, so that the equilibrium average of the kernel given in Eq.(3.9) may also be factored into a product of a longitudinal average and a transverse average [131]: $\langle \mathcal{H} \rangle_{\text{eq}} =$

$\langle \mathcal{H}_{\parallel}(i, j; k_{\parallel}) \rangle_{\text{eq}} \langle \mathcal{H}_{\perp}(i, j; n, m) \rangle_{\text{eq}}$, with

$$\langle \mathcal{H}_{\parallel}(i, j; k_{\parallel}) \rangle_{\text{eq}} \equiv \langle e^{ik_{\parallel}(z_i - z_j)} \rangle_{\text{eq}} \quad (3.10)$$

$$\langle \mathcal{H}_{\perp}(i, j; n, m) \rangle_{\text{eq}} \equiv \langle J_n(\alpha_{nm}\rho_i/R) J_n(\alpha_{nm}\rho_j/R) e^{in(\phi_i - \phi_j)} \rangle_{\text{eq}} . \quad (3.11)$$

The longitudinal equilibrium average obtains trivially. The distribution function in this case is given by the ordinary one-dimensional Gaussian distribution function

$$\psi_{\parallel}(z_i - z_j; |i - j|) = \left(\frac{3}{2\pi|i - j|b^2} \right)^{1/2} \exp \left[-\frac{3(z_i - z_j)^2}{2|i - j|b^2} \right]. \quad (3.12)$$

To find the transverse equilibrium average, we must solve for a two-dimensional Gaussian polymer of N monomer units confined to a disk of radius R . The basic approach is to calculate $\psi_{\perp}(\boldsymbol{\rho}_i, \boldsymbol{\rho}_j; i, j)$, the propagator (Green's function) $G_0(\boldsymbol{\rho}, \boldsymbol{\rho}'; N)$, which gives the statistical weight of a chain starting at $\boldsymbol{\rho}$ and ending at $\boldsymbol{\rho}'$, and then get $\psi_{\perp}(\boldsymbol{\rho}_i, \boldsymbol{\rho}_j; i, j)$ from $G_0(\boldsymbol{\rho}, \boldsymbol{\rho}'; N)$. The propagator is given by the solution to the equation

$$\left(\frac{\partial}{\partial N} - \frac{b^2}{6} \nabla_{\perp}^2 \right) G_0(\boldsymbol{\rho}, \boldsymbol{\rho}'; N) = \delta(\boldsymbol{\rho} - \boldsymbol{\rho}') \delta(N), \quad (3.13)$$

subject to the boundary condition $G_0(\boldsymbol{\rho}, \boldsymbol{\rho}'; N) = 0$ on $\rho = |\boldsymbol{\rho}| = R$. This calculation is straightforward and similar in spirit to many existing calculations of the distribution of a Gaussian polymer between parallel plates [132, 133, 134]. It is customary to rewrite Eq.(3.13) as

$$-\partial_N G = (-b^2 \nabla^2 / 6 + U_{\text{ext}}(\boldsymbol{\rho}) / k_B T) G, \quad (3.14)$$

with $G(\boldsymbol{\rho}, \boldsymbol{\rho}'; 0) = \delta(\boldsymbol{\rho}, \boldsymbol{\rho}')$, because of its remarkable similarity to the Schrödinger equation for a non-relativistic particle.

In some cases we can solve this equation directly. In many other cases, it is more convenient to use an *expansion in eigenfunctions*. We introduce a linear Hermitian operator Γ corresponding to the right-hand side of Eq.(3.14),

$$\Gamma = -\frac{b^2}{6}\nabla^2 + \frac{U_{ext}(\boldsymbol{\rho})}{k_B T} . \quad (3.15)$$

The spectrum of this operator is then obtained from

$$\Gamma u_k(\boldsymbol{\rho}) = \epsilon_k u_k(\boldsymbol{\rho}) , \quad (3.16)$$

where $u_k(\boldsymbol{\rho})$ are its eigenfunctions with eigenvalues ϵ_k , starting from a minimal value ϵ_0 , the ground state. The u_k 's satisfy the usual orthogonality and closure relations.

The explicit form of G is an expansion in these eigenfunctions,

$$G(\boldsymbol{\rho}, \boldsymbol{\rho}'; N) = \sum_k u_k^*(\boldsymbol{\rho}) u_k(\boldsymbol{\rho}') \exp(-N\epsilon_k) . \quad (3.17)$$

The transverse part of the two-point equilibrium distribution function is given by

$$\psi_{\perp,}(\boldsymbol{\rho}_i, \boldsymbol{\rho}_j; |i-j|) = \frac{\int d\boldsymbol{\rho}_0 \int d\boldsymbol{\rho}_N G(\boldsymbol{\rho}_0, \boldsymbol{\rho}_i; i) G(\boldsymbol{\rho}_i, \boldsymbol{\rho}_j; |i-j|) G(\boldsymbol{\rho}_j, \boldsymbol{\rho}_N; |N-j|)}{\int d\boldsymbol{\rho}_0 \int d\boldsymbol{\rho}_N G(\boldsymbol{\rho}_0, \boldsymbol{\rho}_N; N)} . \quad (3.18)$$

The resulting expressions for arbitrary R are complicated and not very useful. However, in the limit of narrow channels ($R < R_{\parallel}$), we may invoke the ground-state dominance approximation [49], and simplify these expressions considerably. In

the ground-state dominance regime, it is permissible to keep only the first term in this eigenfunction expansion since the ratio of the consecutive terms in the expansion is (in our case) of the order of $\exp(-\text{const.}(R_{\parallel}/R)^2)$, which becomes negligibly small when $R/R_{\parallel} \ll 1$. Thus one finds $G_0(\boldsymbol{\rho}, \boldsymbol{\rho}'; N) = \varphi_0(\rho)\varphi_0(\rho') \exp(-\epsilon_0 N)$ and $\psi_{\perp}(\boldsymbol{\rho}_i, \boldsymbol{\rho}_j; i, j) = \varphi_0^2(\rho_i)\varphi_0^2(\rho_j)$, where $\varphi_0(\rho)$ is the solution of ⁸

$$\frac{b^2}{6} \frac{1}{\rho} \frac{d}{d\rho} \left(\rho \frac{d\varphi_0}{d\rho} \right) + \epsilon_0 \varphi_0 = 0, \quad (3.19)$$

subject to $\varphi_0(R) = 0$ and the normalization condition $2\pi \int_0^R d\rho \rho |\varphi_0(\rho)|^2 = 1$. Hence, for very narrow capillaries, we find [131]

$$\langle \mathcal{H}_{\perp}(i, j; n, m) \rangle_{\text{eq}} = \left[2\pi \int_0^R d\rho \rho J_0(\alpha_{0m}\rho/R) \sigma(\rho) \right]^2 \delta_{n0}, \quad (3.20)$$

where $\sigma(\rho) = |\varphi_0(\rho)|^2 = J_0^2(\alpha_{01}\rho/R)/\pi R^2 J_1^2(\alpha_{01})$ is the normalized monomer number density.

Combining these results using Eq.(3.20) for a narrow channel, we obtain

$$D_{\parallel, \Theta} = \frac{2\alpha_{01}^2 k_B T}{\pi^2 N \eta R^8} \left[\int_0^R \left(\frac{J_0(\alpha_{01}\rho/R)}{J_1(\alpha_{01})} \right)^3 \rho d\rho \right]^2 \int_{-\infty}^{+\infty} \frac{g_{\Theta}(k_{\parallel}) dk_{\parallel}}{\left(k_{\parallel}^2 + (\alpha_{01}/R)^2 \right)^2}, \quad (3.21)$$

where the subscript Θ means the theta condition. Carrying out the integrations in Eq.(3.21) with the aid of the Gaussian-chain structure factor gives an estimate of the diffusion constant of the center of mass of a single polymer at Θ conditions and, in the absence of colloids,

$$D_{\parallel} = 0.186 \frac{k_B T}{\eta_s N^{1/2} b}. \quad (3.22)$$

⁸The radial symmetry of φ is a consequence of a general theorem concerning the solution of second-order elliptic partial differential equations [135].

We should point out that the application of the Gaussian model in confined geometries is subject to a number of important caveats. Self-avoidance cannot be entirely ignored for polymers in a Θ solvent in sufficiently narrow capillaries. Furthermore, polymer chains at Θ conditions and in narrow capillaries are expected to form knots, which have been neglected in the present treatment.

3.3 Polymer in a Good Solvent - Swollen Chains

In situations where excluded volume effects are relevant, the calculation of D_{\parallel} using the expressions given in Eqs. (3.8) and (3.9) becomes difficult. As in the case of a self-avoiding polymer in free space, the exact two-point distribution function $\Psi_{\text{eq}}(\mathbf{r}_i, \mathbf{r}_j)$ of a confined self-avoiding polymer is unknown. Moreover, the factoring of the distribution function into a product of longitudinal and transverse two-point functions is in general not possible. The best one may do is to obtain the scaling properties of the averages in Eq.(3.9) by, for instance, renormalization group calculations. Theoretical predictions for D_{\parallel} based on scaling arguments give $D_{\parallel} \sim N^{-1}(R/b)^{2/3}$ [136]. These scaling theories are in good qualitative agreement with experimental studies [137], but are unable to predict the numerical prefactors.

Alternatively, estimates of these averages that include numerical prefactors may be achieved using self-consistent approximation schemes. Variational approaches or

self-consistent mean-field theories have been successfully used in certain problems under unconfined conditions [138, 139]. But such approaches are in general quite involved, especially in confined geometries. However, in *strongly* confined systems, they can be sufficiently simplified to facilitate calculations. For very narrow capillaries, breaking of the averages into longitudinal and transverse components is a reasonable approximation. Thus we may estimate D_{\parallel} , with ψ_{\parallel} and $\sigma(\rho)$ appropriate for excluded-volume chains.

The calculational method for obtaining $\sigma(\rho)$ is analogous to that employed in the previous case. In a self-consistent mean-field treatment, the propagator satisfies Eq.(3.13), augmented by a mean-field potential proportional to the local monomer concentration, $U(\mathbf{r}) = \nu k_B T c(\mathbf{r}) \simeq \nu k_B T \bar{\lambda} \sigma(\rho)$,

$$\left(\frac{\partial}{\partial N} - \frac{b^2}{6} \nabla_{\perp}^2 + \nu_{eff} \sigma(\rho) \right) G(\boldsymbol{\rho}, \boldsymbol{\rho}'; N) = \delta(\boldsymbol{\rho} - \boldsymbol{\rho}') \delta(N), \quad (3.23)$$

where $\nu_{eff} = \nu \bar{\lambda}$, in which $\bar{\lambda}$ is the linear density of the chain assumed to be constant over the length of the chain. We also require $G(\boldsymbol{\rho}, \boldsymbol{\rho}'; N) = 0$ on $\rho = R$, and $\sigma(\rho)$ to be determined self-consistently from $G(\boldsymbol{\rho}, \boldsymbol{\rho}'; N)$ by

$$\sigma(\rho) = \frac{\int d\boldsymbol{\rho}_0 \int d\boldsymbol{\rho}_N \int_0^N dn G(\boldsymbol{\rho}_0, \boldsymbol{\rho}; N-n) G(\boldsymbol{\rho}, \boldsymbol{\rho}_N; n)}{\int d\boldsymbol{\rho}_0 \int d\boldsymbol{\rho}_N G(\boldsymbol{\rho}_0, \boldsymbol{\rho}_N; N)}. \quad (3.24)$$

For narrow channels, we can reduce Eqs.(3.23) and (3.24) to a single ordinary differential equation, and write an equation similar to Eq.(3.25) with an additional

term

$$\frac{b^2}{6} \frac{1}{\rho} \frac{d}{d\rho} \left(\rho \frac{d\varphi_0}{d\rho} \right) + \epsilon_0 \varphi - \nu_{eff} |\varphi|^2 \varphi = 0, \quad (3.25)$$

subject to the same boundary and normalization conditions. This nonlinear ordinary differential equation may be solved numerically or, for sufficiently small ν_{eff} , perturbatively. Alternatively, it may be recast as a variational integral

$$I = \int_0^R d\rho \rho \left[\frac{b^2}{6} |\nabla_{\perp} \varphi(\rho)|^2 - \epsilon_0 |\varphi(\rho)|^2 + \frac{\nu_{eff}}{2} |\varphi(\rho)|^4 \right], \quad (3.26)$$

which is then minimized for a suitable class of trial functions, $\varphi_{tr}(\rho; \vartheta_i)$, with respect to the variational parameters ϑ_i . With a judicious choice of trial functions, this approach often yields good approximate solutions [49]. Given a solution for $\varphi(\rho)$, we then find $\sigma(\rho)$ from $\sigma(\rho) = |\varphi(\rho)|^2$. In general $\sigma(\rho)$ is a monotonically decreasing function of ρ , and is expected to have a broader distribution compared to the Gaussian case due to the excluded-volume interactions. A commonly proposed form of the trial function, based on the above and some other arguments, is $\varphi_{tr} = A \tanh[(R - \rho)/\xi]$. Therefore, we must solve $\delta I/\delta A = 0$ and $\delta I/\delta \xi = 0$. Eliminating A between the two equations gives $\xi = 0.227b(R/b)^{3/4}$ for athermal solvents ($\nu = b^3$). A is then obtained separately from the normalization condition for φ_{tr} and is given by $[2\pi \int_0^R [\tanh((R - \rho)/\xi)]^2 \rho d\rho]^{-1/2}$.

The structure factor of a self-avoiding chain cannot be computed exactly. However, for sufficiently narrow capillaries, the chain is in a strongly extended state, leading to a uniform linear density of the monomers except perhaps near the ends of the chain. Assuming $\lambda(z) = \langle \lambda(z) \rangle_{eq}$ gives an approximate closed-form expression for the

structure factor [140]. With $g(k_{\parallel})$ in hand, the diffusion constant along the axis of the capillary can be obtained from

$$D_{\parallel, G} = \frac{\alpha_{01}^2 k_B T}{2\pi^2 N \eta R^4} \left[\int_0^R \frac{J_0(\alpha_{01}\rho/R)}{J_1(\alpha_{01})} A^2 \tanh^2 \left(\frac{R-\rho}{\xi} \right) \rho d\rho \right]^2 \int_{-\infty}^{+\infty} \frac{g_G(k_{\parallel}) dk_{\parallel}}{\left(k_{\parallel}^2 + (\alpha_{01}/R)^2 \right)^2}, \quad (3.27)$$

where the subscript G means good solvent condition.

3.4 Single Polymer with Many Colloids

Addition of colloids to the system of polymer+solvent in a quasi-one-dimensional channel (see Fig.3.1) makes the problem of polymer dynamics more challenging, and renders the solution from first principles a tremendously difficult task.

The idea we use here is based on a physical picture of a diffusing polymer in which the dominant mode of transport is cage diffusion [25]: the polymer tries to escape from the dynamic cage created by its two neighboring colloids. Our starting point is Eq.(3.7) for the diffusion of the polymer's center of mass. It corresponds to the diffusion coefficient obtained from the initial decay rate in intensity of the scattered light in scattering experiments, and therefore gives the short-time diffusion coefficient. For short times, the polymer is still trapped inside the cage and merely rattles between the colloids. During this time, the colloids, which are much larger than the monomers, have hardly moved. Thus we will neglect their influence on the hydrodynamic motion of monomers. However, the two neighboring colloids act as

barriers against the motion of the chain. As a first approximation, the associated barrier potential for the two colloids, located a distance L apart, may be described by a combination of delta functions (see Fig.3.2)

$$\beta U(z) = \frac{1}{2} S(a, R, b) [\delta(z - L/2) + \delta(z + L/2)] , \quad (3.28)$$

where we assume that the channel is in the z -direction, and where S is the strength of the barrier, which depends on the size of colloids and monomers as well as the diameter of the cylinder. Roughly speaking, the strength of this entropic barrier for a monomer is inversely proportional to the area accessible to it. Therefore $S \propto b^2/(R^2 - a^2)$. On the other hand, S has the dimensions of length and has to vanish as $a \rightarrow 0$. These arguments suggest the following ansatz for S

$$S \sim \frac{a(b/R)^2}{1 - (a/R)^2} , \quad (3.29)$$

To proceed further, knowledge of the structure factors is called for. When the chain is subject to an external potential $U(z)$, the average monomer concentration at position z' will change from $\bar{\lambda}$ to $\bar{\lambda} \exp[-\beta U(z')]$, and thus the net difference is $\bar{\lambda} [\exp(-\beta U(z')) - 1]$. However, since the monomers are interconnected, this will also affect the local concentration at position z by an amount given by the correlation of the monomers located at those two points, i.e., by $g(z - z')$. The final expression for the pair correlation function in the case of a weak external potential reads [49]

$$g(z) - g^0(z) = - \int g^0(z - z') \bar{\lambda} \beta U(z') dz' , \quad (3.30)$$

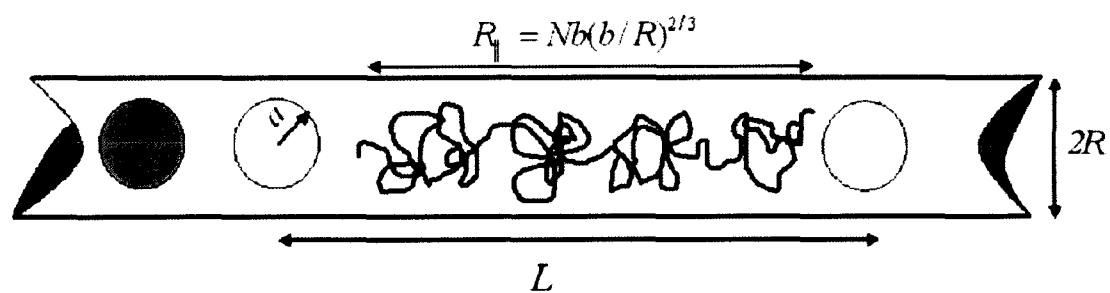


Figure 3.1: Schematic representation of a polymer chain confined in a narrow channel and trapped between two colloids (the neighboring colloids are in yellow).

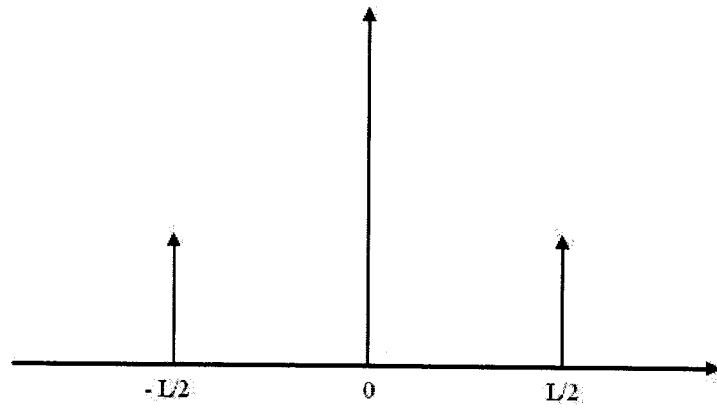


Figure 3.2: Schematic representation of the barrier potential used in Eq.(3.28).

where $g^0(z)$ is the pair correlation function in the absence of the external potential. Needed to compute the diffusion constant is the Fourier transform of $g(z)$. Performing this Fourier transform, using the convolution property in Eq.(3.30) with the above barrier potential, gives for the structure factor

$$g(k_{\parallel}) = g^0(k_{\parallel})[1 - \alpha \cos(k_{\parallel}L/2)] , \quad (3.31)$$

with $\alpha = \bar{\lambda}S$ ($0 \leq \alpha \leq 1$). This relation gives the diffusion coefficient for a particular configuration of the two neighboring colloids separated by a distance L , which then has to be averaged over all possible distances using the nearest-neighbor distribution function of colloids, $H(L)$. Fortunately, $H(L)$ is exactly known for pure colloids modeled as hard spheres (hard rods) in one dimension [141], and the presence of a single polymer in a dilute solution will not change this distribution significantly:

$$2aH(L) = \kappa \exp[-\kappa(L/2a - 1)] , \quad (3.32)$$

where $\kappa = 2\eta_c/(1 - \eta_c)$, with η_c the packing fraction of colloids in the channel.

Fig.3.3 and Fig.3.4 show the normalized diffusion coefficient of a polymer in theta and good solvents respectively, and for several values of the parameter α . As expected, the diffusion coefficient decreases with increasing colloids packing fraction and with increasing the extent of confinement. For fixed values of κ and α the polymer has a higher diffusion coefficient in the theta solvent than in the good solvent. This has to do with the constraint of self-avoidance in the good solvent condition. The confinement suppresses the number of possible conformations. The suppression has a greater impact on a swollen chain compared to an ideal one.

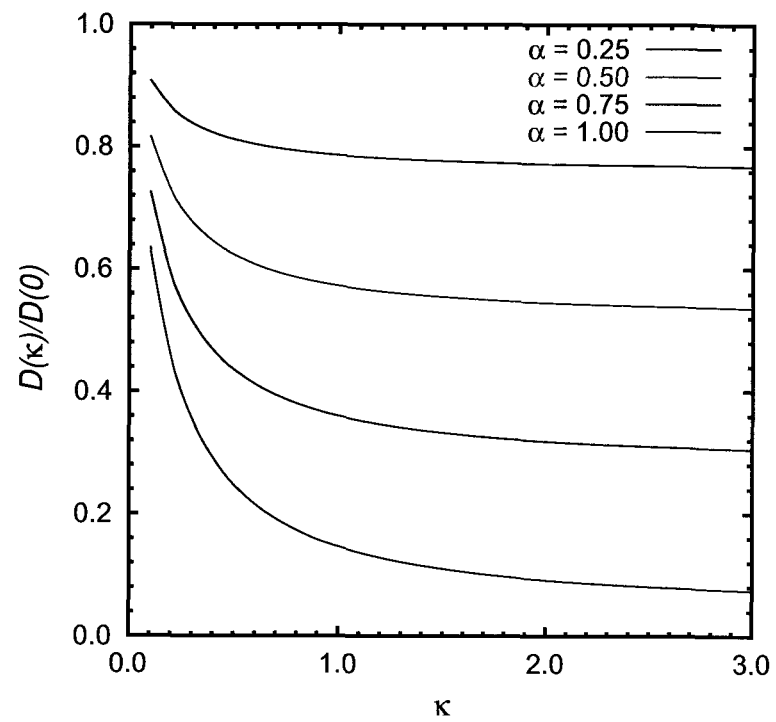


Figure 3.3: Normalized self-diffusion of an ideal polymer chain in a colloidal suspension as a function of colloids packing fraction for various extents of confinement measured by α .

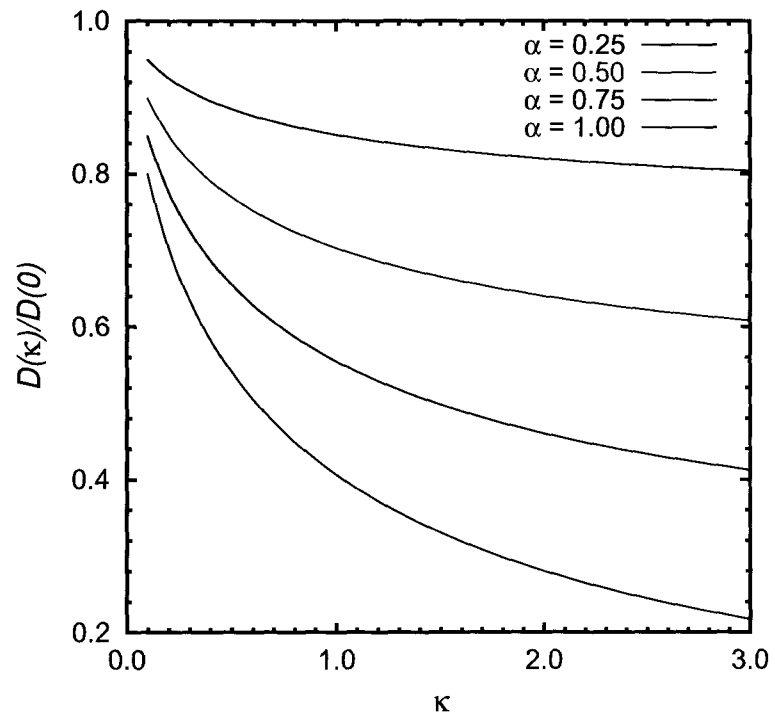


Figure 3.4: Normalized self-diffusion of a swollen polymer chain in a colloidal suspension as a function of colloids packing fraction for various extents of confinement measured by α .

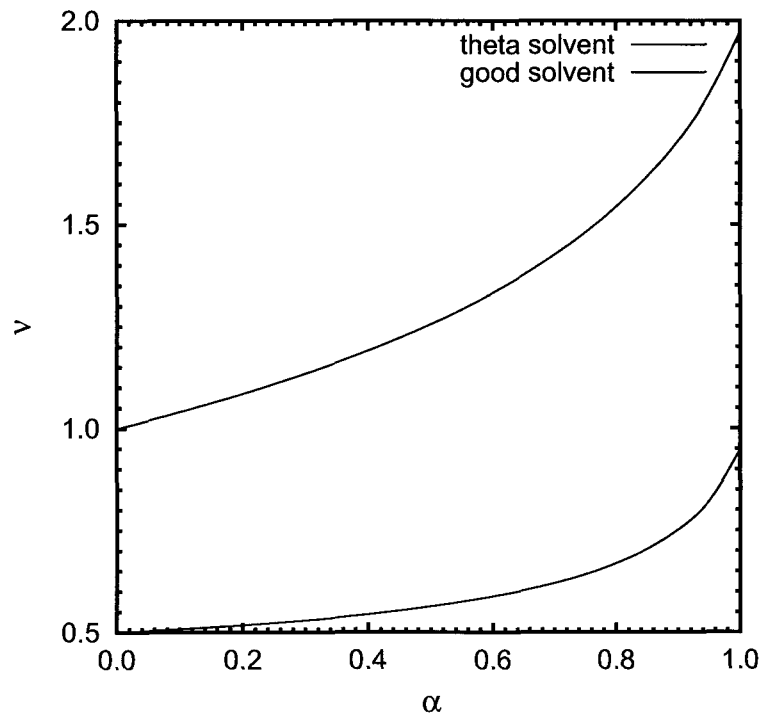


Figure 3.5: Scaling exponent ν in $D \sim N^{-\nu}$ for ideal and swollen chains as a function of colloids packing fraction for various extents of confinement measured by α .

The dependence of the diffusion coefficient on polymerization index (number of monomers) is shown in Fig.3.5. The diffusion coefficient scales with N in a power-law fashion (for large N) with a scaling exponent ν which depends on α . At $\alpha = 0$, the exponents are essentially those of a single chain trapped in a narrow channel in the absence of colloids. The exponent increases with α and reaches a maximum value at $\alpha = 1$ where the chain is under strong confinement. Thus, according to our model the upper bound for ν is about 1 for theta and about 2 for good solvent conditions.

To check for consistency, we need to obtain the conditions that keep α less than unity. Since $\bar{\lambda} = N/R_{\parallel} \simeq b^{-1}(b/R)^{-2/3}$ and $S \sim a(b/R)^2$, we find that α scales like $(b/R)^{1/3}$, assuming $a/R = O(1)$. This means that the value of α will be less than unity as long as the prefactor that appears in Eq.(3.29) (to make it an equality) is itself of the order of unity. Nevertheless, this argument breaks down when R gets extremely close to a . One way to resolve this issue is to realize that the diffusion constant scales with the size of the channel, suggesting that by enforcing the scaling condition, we can obtain the dependencies of α and S on R for both the ideal (Θ solvent) and the real chains (good solvent).

We explicate the steps in the case an ideal polymer, since we essentially have to follow similar steps in the case of a real chain. First, let us define f and f^0 as:

$$f(R, L) = \int_0^{\infty} g^0(x) [1 - \alpha(R) \cos(xL/R_{\parallel})] dx \quad (3.33)$$

$$f^0 = \int_0^{\infty} g^0(x) dx, \quad (3.34)$$

where $R_{\parallel} = (2/\sqrt{6})N^{1/2}b$ is twice the radius of gyration of an ideal polymer. The

R -dependence of the diffusion constant pertaining to the addition of colloids comes from the ratio f/f^0 . Therefore, if D_{\parallel} is to scale with R according to a power-law, then the second derivative of the logarithm of this ratio with respect to the logarithm of R , after taking the appropriate statistical average, has to vanish, i.e., $\partial^2 \ln(\bar{f}/f^0)/\partial(\ln R)^2 = 0$, in which \bar{f} is the average of f over all possible distances L between two neighboring colloids. Note that the measured exponent in actual experiments is usually expressed as a function of the concentration of the colloidal suspension, and not of the average distance between the colloids, since the former is known in advance. Imposing this condition yields for \bar{f}

$$\bar{f} = \int_{2a}^{\infty} f(R, L)H(L, \kappa)dL = CR^{\omega} , \quad (3.35)$$

where ω and C are arbitrary constants. On the other hand, at the Θ condition, f can be written as

$$f_{\Theta}(R, L) = f_{\Theta}^0 - \alpha(R)p_{\Theta}(L) = f_{\Theta}^0 - \alpha_{\Theta} \int_0^{\infty} g_{\Theta}^0(x) \cos(xL/R_{\parallel})dx , \quad (3.36)$$

where the subscript Θ stands for the theta solvent condition. Setting these two expressions equal to each other, subject to the boundary condition $\alpha(a) = 1$, gives

$$\alpha_{\Theta} = (R/a)^{\omega_{\Theta}} + \frac{f_{\Theta}^0}{\bar{p}_{\Theta}} (1 - (R/a)^{\omega_{\Theta}}) , \quad (3.37)$$

where $\bar{p}_{\Theta} = \int_{2a}^{\infty} p(L)H(L, \kappa)dL$. ω_{Θ} has to be determined from the fact that at a certain radius R^* , a monomer hardly feels the effect of the colloid as a one-dimensional obstacle along the direction of motion. This is when the transition to three dimensions

occurs at which $\alpha(R^*) = 0$, and the polymer retrieves its original conformation in free space. In terms of this critical value of the channel radius, we will have

$$\alpha_{\Theta} = (\bar{p}_{\Theta})^{-1} \left[f_{\Theta}^0 - (f_{\Theta}^0 - \bar{p}_{\Theta}) \left(\frac{f_{\Theta}^0}{f_{\Theta}^0 - \bar{p}_{\Theta}} \right)^{\frac{\ln(R/a)}{\ln(R^*/a)}} \right], \quad (3.38)$$

with the exponent $\omega_{\Theta} = \ln(f_{\Theta}^0/(f_{\Theta}^0 - \bar{p}_{\Theta}))/\ln(R^*/a)$. A similar expression can be developed for a real (swollen) chain. The minor differences compared to the expression obtained above is due to the dependence of R_{\parallel} on R . This means that now $p_G = p_G(L, R)$, which leads to:

$$\alpha_G = (\bar{p}_G(R))^{-1} \left[f_G^0 - (f_G^0 - \bar{p}_G(1)) \left(\frac{f_G^0}{f_G^0 - \bar{p}_G(1)} \right)^{\frac{\ln(R/a)}{\ln(R^*/a)}} \right], \quad (3.39)$$

with the exponent $\omega_G = \ln(f_G^0/(f_G^0 - \bar{p}_G(1)))/\ln(R^*/a)$ in which

$\bar{p}_G(R) = \int_{2a}^{\infty} p_G(L, R)H(L, \kappa)dL$, and the subscript G stands for the good solvent condition.

For both ideal and real chains, the exponent ω increases with the concentration of colloids, and decreases with the critical radius (R^*) of the channel (Fig.3.6 and Fig.3.7). Although this radius is unknown⁹, an upper bound for ω is achieved by inserting $R^* = 2a$ into the above equations. However, there are some evidence [126] that the crossover to two dimensions does not occur for $R < 4a$. The exponent ω saturates at high values of κ for both ideal and real chains showing a much stronger dependence on the concentration of colloids in the case of real chains. At $\kappa = 0$ we recover the values known for a single chain in a narrow channel in the absence of colloids, i.e., $\omega = 0$ for theta and $\omega \approx 0.6$ for good solvent conditions.

⁹It is of the order of magnitude of the Flory radius.

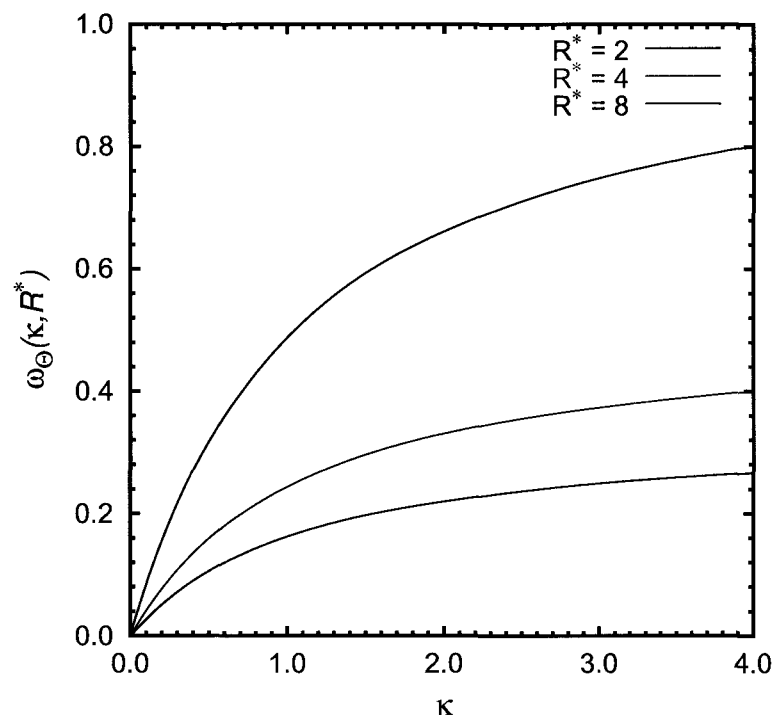


Figure 3.6: Exponent ω in $D \sim R^\omega$ for an ideal chain in a colloidal suspension as a function of the concentration of colloids and for different values of the critical radius R^* (in units of $2a$).

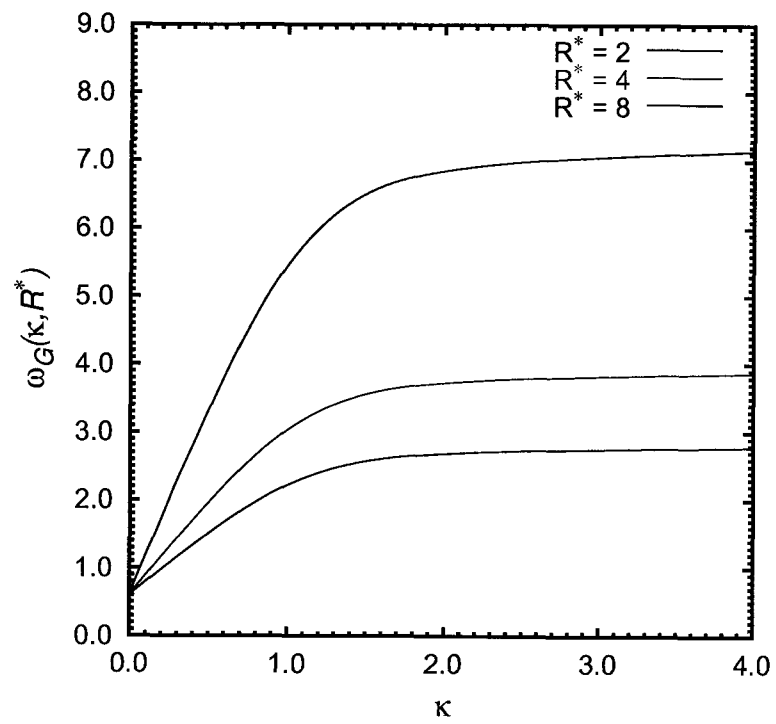


Figure 3.7: Exponent ω in $D \sim R^\omega$ for a real chain in a colloidal suspension as a function of the concentration of colloids and for different values of the critical radius R^* (in units of $2a$).

Next, we consider another ansatz for the barrier potential that takes the widths of the barrier into account, in order to investigate the sensitivity of the results to the shape of the potential. We choose a repulsive square-wall potential, whose width is of the order of the colloid diameter, and which can be represented by (see Fig.3.8)

$$\beta U(z) = \frac{1}{2}\tilde{S}[\Theta(z-(L/2-a))-\Theta(z-(L/2+a))] + \frac{1}{2}\tilde{S}[\Theta(z+(L/2+a))-\Theta(z+(L/2-a))] , \quad (3.40)$$

where $\Theta(z)$ is the Heaviside step function and \tilde{S} is the strength of the barrier (dimensionless in this case). Following the same procedure as above, we obtain

$$g(k_{\parallel}) = g^0(k_{\parallel})[1 - 2\tilde{\alpha}k_{\parallel}^{-1} \sin(k_{\parallel}a) \cos(k_{\parallel}L/2)] , \quad (3.41)$$

with $\tilde{\alpha} = \bar{\lambda}\tilde{S}$. Although this result for the structure factor is somewhat different from the earlier one, it will give essentially the same value for D_{\parallel} by simply rescaling the strength of the barrier potential. The reason for this lies in the fact that most of the contribution in the last integral appearing in Eq.(3.21) or Eq.(3.27) comes from values of $k_{\parallel}R_{\parallel} \lesssim 1$, which means $k_{\parallel}R \ll 1$. This allows us to safely neglect the higher-order terms in the Taylor expansion of $\sin(ka)$ about zero. Thus the above expression for $g(k_{\parallel})$ will eventually reduce to that of Eq.(3.31) if $S \equiv 2a\tilde{S}$.

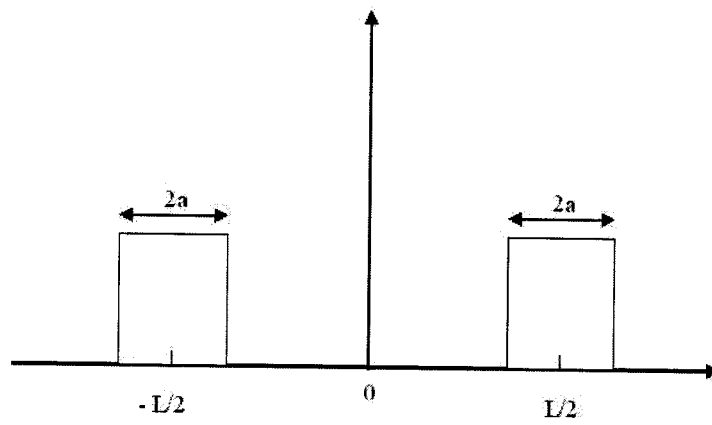


Figure 3.8: Schematic representation of the barrier potential used in Eq.(3.40).

Chapter 4

Phase Transitions of Colloid-Polymer Mixtures in Two Dimensions

This chapter first describes the methods and results of our experimental studies of the phase transitions of mixtures of spherical colloids and polymers trapped at the air-water interface. A set of surface pressure-area isotherms (two-dimensional analog of $p - V$ isotherms) are obtained as a result of these measurements using a Langmuir-Blodgett trough. Next, we present and examine a possible way to explain the experimental observations based on the extension of McMillan's mean-field theory to two-dimensional systems.

4.1 Materials and Experimental Methods

High-molecular weight polymer, poly(L-lactic acid) (PLA), $M = 700,000$, with polydispersity of 1.8, was purchased from Polysciences Inc., in form of small pellets, and was used as received. The radius of gyration of PLA corresponding to the above molecular weight is about 77nm. For the colloids, we used two types of spherical particles: paramagnetic Fe_2O_3 beads coated with short chains of poly(acrylic acid) 790 nm in diameter, and Cd-Se nanoparticles 4-5 nm in diameter.

To prepare the samples, colloidal particles and polymer are both dissolved in chloroform at room temperature. In the case of PLA, even after shaking and stirring with a vortex creator, it takes tens of minutes for the pellets to get completely dissolved. The Langmuir-Blodgett trough is cleaned thoroughly with isopropyl alcohol and acetone at the beginning of each experiment, and rinsed under deionized water. Impurities, dust particles, and other contaminants that might be present on the surface of the subphase (water in this case) or edges of the barriers, must also be removed. This is simply done by slowly scanning the water surface and sucking any possible dirt with a pipet tip connected to the suction section of a small pump. With the help of a mini syringe, samples are then spread onto the water surface of a standard Langmuir-Blodgett trough (900 cm², KSV instruments Ltd.), filled with ultrapure (resistivity = 18.2 M Ω .cm) water obtained by passing tap water through a Millipore water purification system. Typically, the suitable amount of sample being used which gives a uniform spreading depends on the materials, and is in fact a matter

of trial and error. In our case, this is between 100 and 200 μl .

We then wait between 15 to 20 minutes before starting to perform measurements, to ensure that the solvent has completely evaporated. This can be verified by monitoring the surface tension of the sample as the evaporation proceeds. The effective area of the trough is changed by moving the two barriers placed symmetrically at both ends of the trough. A Schematic of the system is shown in Fig.4.1.

As the sample goes through successive compression-expansion cycles, a sensitive Wilhelmy plate (0.004 mN/m resolution), dipped about halfway into the water subphase, records the excess surface tension (with respect to the subphase) caused by the sample molecules floating at the surface. In order to get reliable data, the plate has to be positioned in a direction perpendicular to the barriers. The trough can be connected to a heat exchanger (external bath) coupled to an on/off simple system, in order to control the temperature of the subphase, by circulating water or glycol through the base of the trough. Temperatures between 0°C and 60°C are achievable in this way.

The rate at which the barriers sweep the air-water interface is set to 10 mm/min, and is chosen such that the molecules have enough time to respond to the changes in area, so that the measured surface tension (pressure) represents the equilibrium value.

Both colloidal particles used in the experiments are sterically stabilized, partially hydrophobic, and neutral. PLA, on the other hand, is hydrophobic along its backbone,

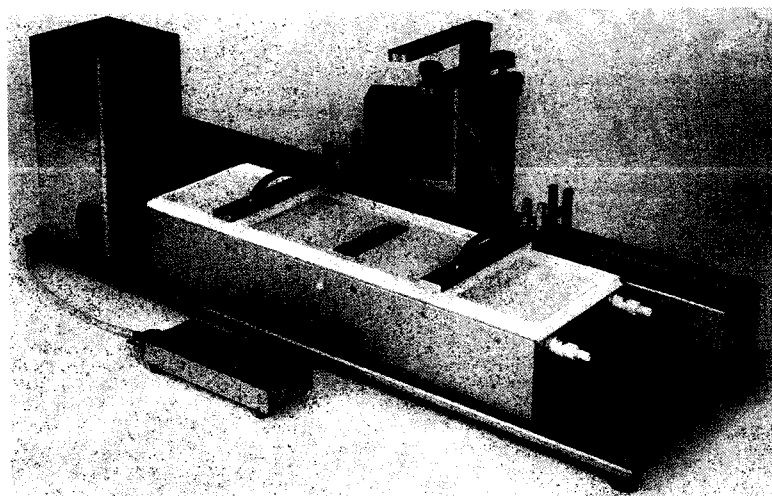


Figure 4.1: Langmuir-Blodgett trough, KSV 2000 series.

with strong hydrophilicity due to the carboxyl groups. This gives PLA an amphiphilic character which allows it to adopt purely two-dimensional conformations at the air-water interface. In addition, when sufficiently compressed, it spontaneously forms 10_3 ¹⁰ helices at the air-water interface. Studies [142, 143] show that the helical structure withstands compression up to the solid-like state, and reduction of surface area merely changes the type of the helix from 10_3 to 3_1 . This property distinguishes PLA from most other polymers, which can only remain flat at the air-water interface over a narrow range of concentrations. Further compression (increase in concentration) will lead to either buckling and formation of multilayers, or flipping up of monomer units.

First, we investigate the pressure(π)-area(A) isotherms for the one-component systems of pure colloids and pure polymers. Both the magnetic colloids and the nanoparticles exhibit no transition up to the onset of monolayer collapse and the emergence of multilayers (see Fig.4.2). The isotherms of PLA, however, exhibit a plateau (Fig.4.3), in accord with the experiments of Esker, et al. [144]. This plateau is due to a structural phase transition from the liquid-expanded (LE) to the liquid-condensed (LC) states. Brewster-angle microscopy reveals [144] that at the transition surface pressure, islands of PLA molecules, ordered into a lamellar pattern, are condensed out of the original disordered liquid state. It is important to realize that these patterns are different from the lamellar structures arising from phase separation of block-copolymers, in the sense that there are no folded chains in a PLA lamella.

¹⁰Crystallographic nomenclature; in a 10_3 helix, 3 turns are required to make a helix consisting of 10 residues.

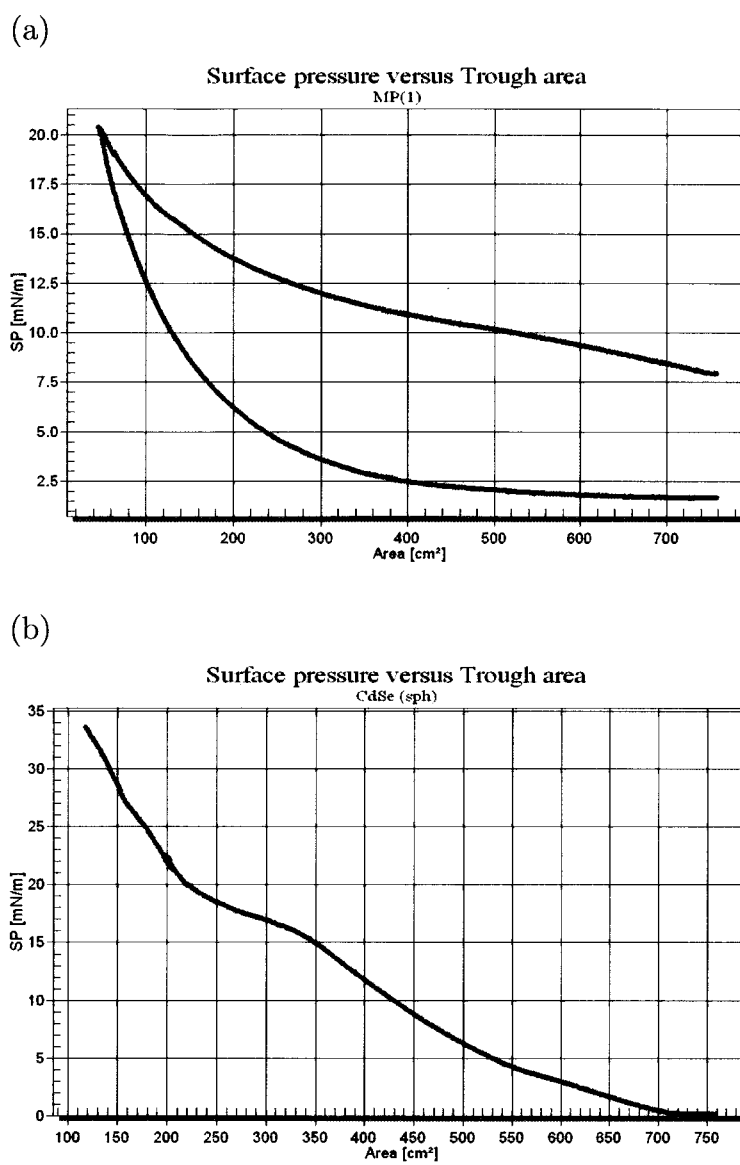


Figure 4.2: $\pi - A$ isotherm for pure colloidal particles at 14.2°C; (a) Magnetic colloids; (b) Cd-Se nanoparticles.

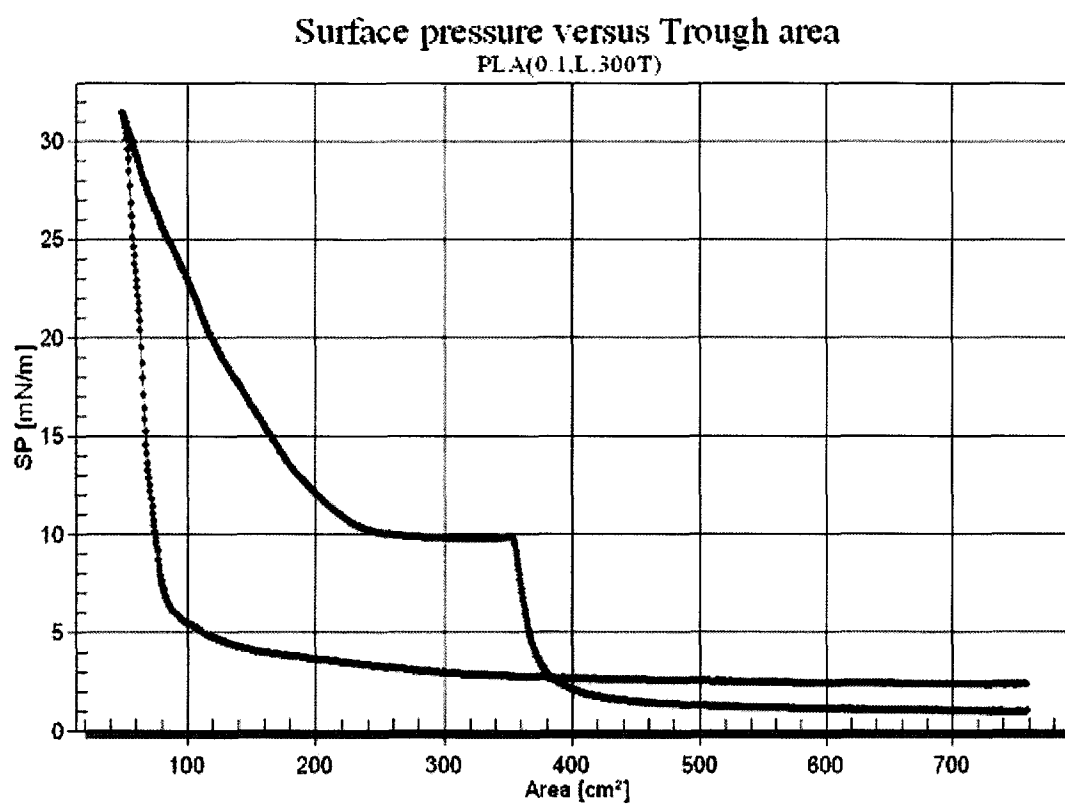


Figure 4.3: $\pi - A$ isotherm for pure PLA molecules at 14.2°C.

In this regard, the patterns are reminiscent of a smectic phase of rigid rodlike polymers or of small liquid-crystalline molecules [145].

The nearly vanishing slope of the curve for the entire transition region (see Fig.4.3) supports a first-order transition. This is in agreement with the fact that the isotropic-smectic phase transition is first-order, and the plateau cannot be accounted for by an isotropic-nematic transition, which is generally continuous in two dimensions ¹¹.

4.2 PLA-Particle Mixtures

We next investigate the influence on the LE-LC transition of adding colloidal particles and the possible emergence of new coexisting phases similar to what has been observed in bulk solutions during liquid-liquid phase separation [147]. We look at two limiting cases:

1. Colloid limit: magnetic colloid + PLA ($q \approx 0.2$)
2. Protein limit: nanoparticle + PLA ($q \approx 32$)

where q is the polymer-to-colloid size ratio.

To perform the experiments, we prepare mixtures of colloids (magnetic particles and nanoparticles) and polymers (PLA) dissolved in chloroform at the desired concentrations, and of equal volumes. Therefore, after mixing the two components, the final concentrations of each of the component will be in fact half of what has been

¹¹The isotropic-nematic transition can be first -order in two dimensions if the anisotropic part of the intermolecular interactions is sufficiently sharp and narrow; see for example [146].

initially prepared. Finding the suitable concentrations is again a matter of experience, and some trial and error. If the solution is too dilute, no phase transition will occur, whereas if it is too concentrated, it will form a solid-like elastic film before compression starts.

Mixtures of Magnetic Colloids and PLA

As can be seen in Fig.4.4, addition of magnetic colloids to PLA reduces the width of the LE-LC transition. For a fixed value of the PLA concentration, there is a critical colloid density at which the LE-LC phase transition disappears. Raising the temperature above a critical value has a similar effect [144]; in this respect, the density of colloids plays the role of temperature. Furthermore, upon addition of colloidal particles, the surface pressure at which the LE-LC transition occurs does not change significantly; however the area corresponding to the onset of the transition shifts to lower values.

These observations can be explained qualitatively by observing that the presence of colloids will increase the average distance between the PLA molecules, and in order for the PLA molecules to feel each other (either through direct interactions, or through entropic effects such as packing), the area available to the mixture has to decrease. On the other hand, colloidal particles make it more difficult for large clusters of PLA molecules to form ordered lamellar structures, and therefore if the density of the colloids is high enough, no such cluster will appear in the system.

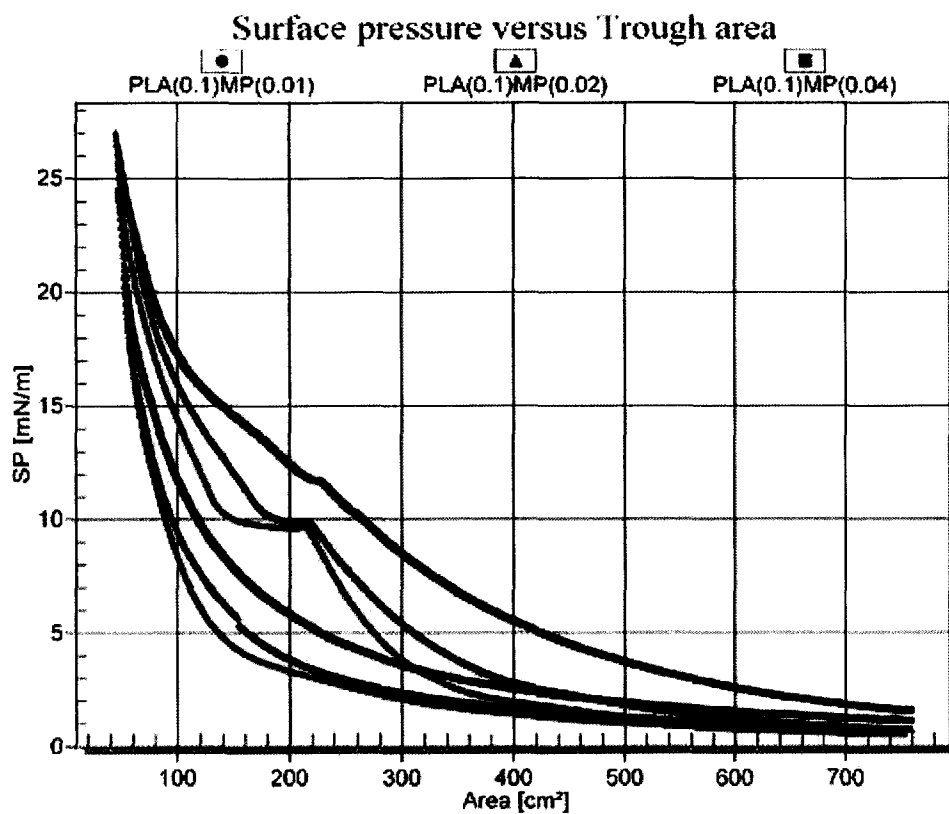


Figure 4.4: $\pi - A$ isotherm for mixtures of PLA and magnetic colloids at three different concentrations. The top values in brackets are the concentrations of each component in units of mg/ml.

Mixtures of Nanoparticles and PLA

Nanoparticles, even at relatively high concentrations, do not affect the LE-LC transition of PLA (Fig.4.5). Indeed, the lamellar spacing is much larger than the size of individual nanoparticles, which allows nanoparticles to disperse between the PLA molecules without altering the lamellar structure. Fig.4.6 shows that when the concentration of PLA is low, one essentially gets isotherms very similar to those of pure nanoparticles. A plateau in the isotherm will emerge at $\pi = 10\text{mN/mm}$ upon increasing the concentration of PLA, which is the signature of a LE-LC transition in PLA (see Fig.4.7).

Another possibility for the formation of a macroscopic phase upon addition of nanoparticles is when the mixture separates into colloid-rich and polymer-rich phases. However, such liquid-liquid demixing was not observed in our experiments¹². It is plausible that the polymer-to-colloid size ratio of $q \approx 32$ which lies in the protein limit is too large, as intuition suggests that depletion effects in that regime vanish.

Obtaining isotherms for PLA-nanoparticle mixtures with larger nanoparticles and low-molecular weight PLA, leading to a smaller q value (still in the protein limit) is currently undertaken in our group. Note that capillary interactions, which originate from the distortion of the meniscus due to the presence of colloids, are negligible for submicron particles [71]. Also, there is no electrostatic repulsion between the nanoparticles since they are neutral.

¹²Similar results were achieved in computer simulations performed previously in our group (see [102]).

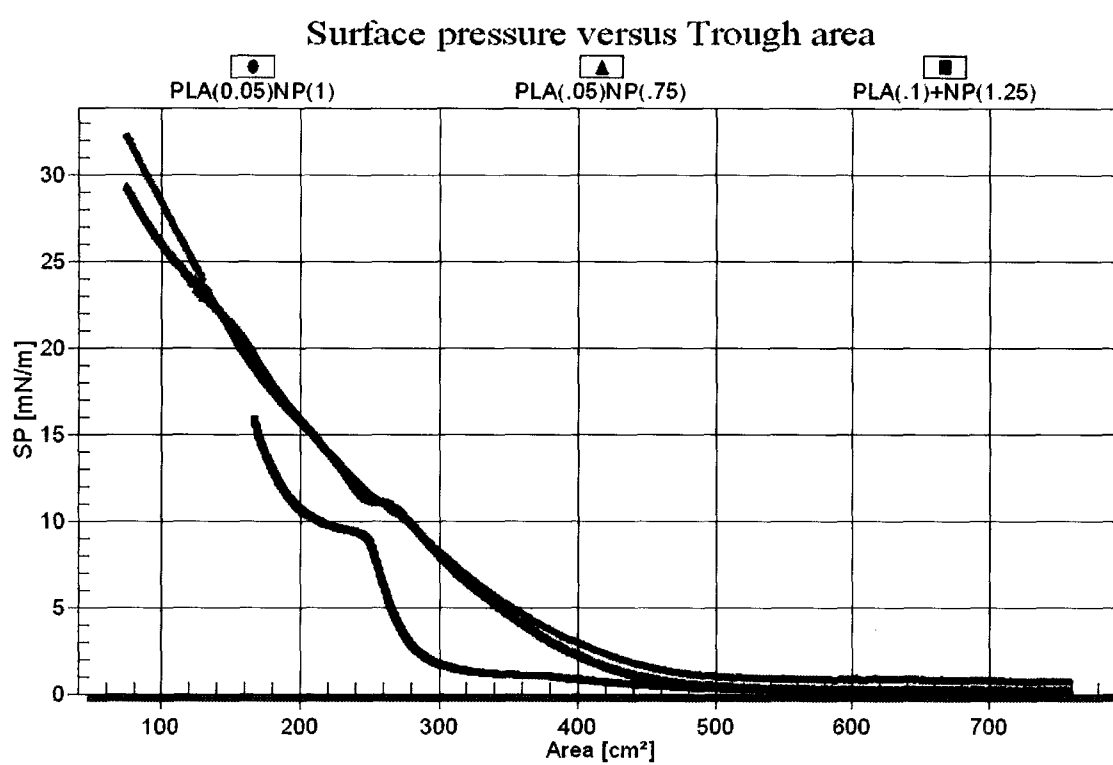


Figure 4.5: $\pi - A$ isotherm for mixtures of PLA and nanoparticles at high nanoparticle concentration. The top values in brackets are the concentrations of each component in units of mg/ml.

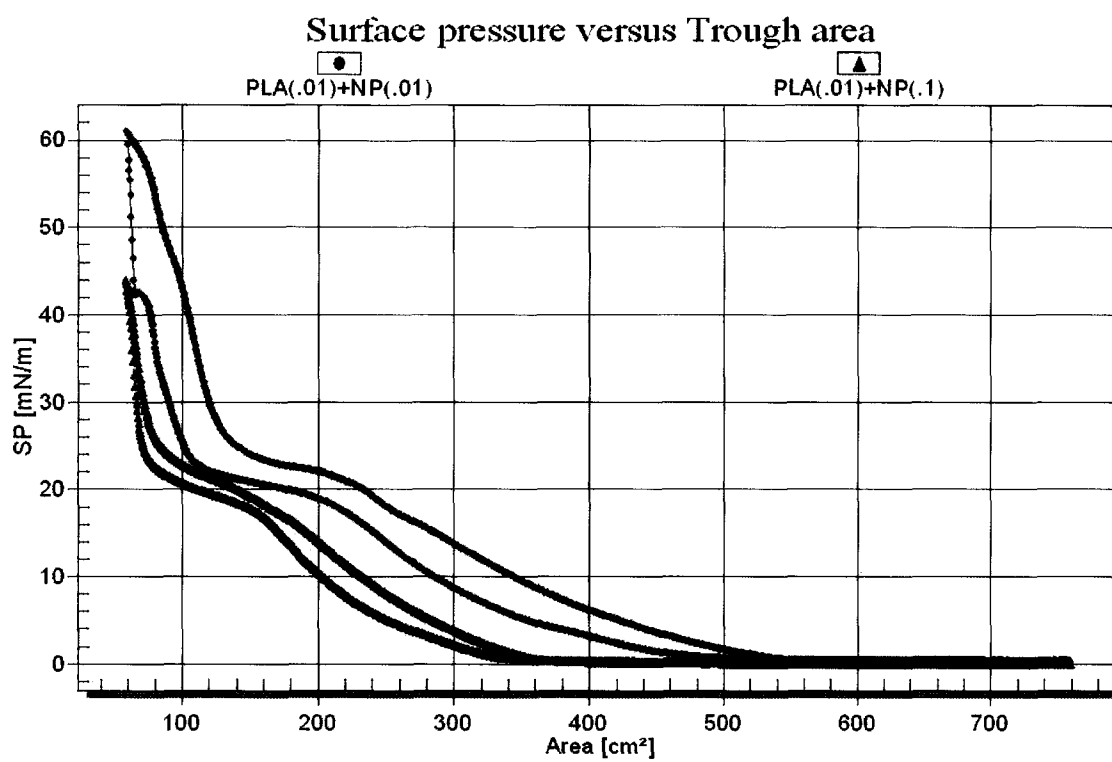


Figure 4.6: $\pi - A$ isotherm for mixtures of PLA and nanoparticles at low PLA concentration. The top values in brackets are the concentrations of each component in units of mg/ml.

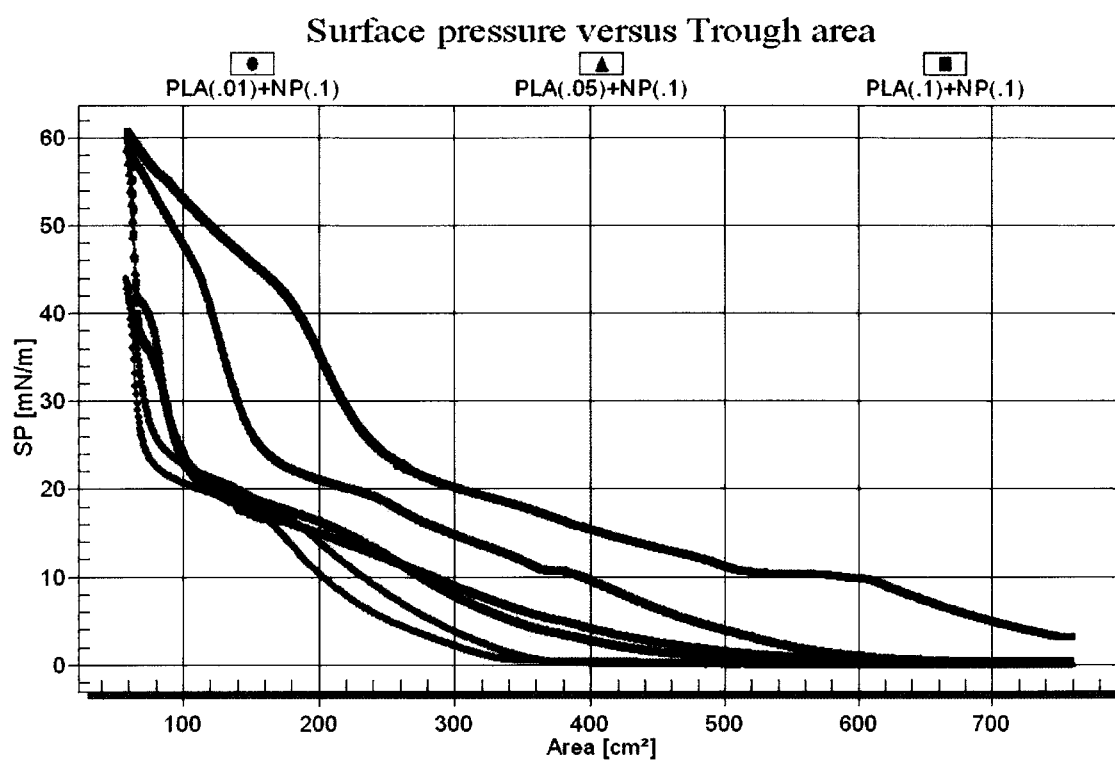


Figure 4.7: $\pi - A$ isotherm for mixtures of PLA and nanoparticles at fixed nanoparticle concentration. The top values in brackets are the concentrations of each component in units of mg/ml.

4.3 McMillan Theory of Smectic-A Phase in Two Dimensions

Straley [148] has shown that true orientational long-range order cannot exist for two-dimensional systems at the thermodynamic limit (infinite system) if the particle interactions are separable into positional and orientational parts. In many systems, including that of hard rods, the positional and orientational parts of the potential are not separable. This allows for the possibility of having orientational long-range order at the thermodynamic limit. However, in the case of hard spherocylinders with variable aspect ratios (from hard disks to hard needles), computer simulations [149] have demonstrated the nematic-isotropic transition is continuous and occurs via a Kosterlitz-Thouless mechanism involving unbinding disclinations. The orientational correlation functions decay algebraically rather than exponentially with distance, implying the absence of true long-range orientational order.

Furthermore, the existence of true translational order, and therefore a true crystalline solid, is ruled out for power-law potentials of the Lennard-Jones type [150]. In this respect, the nematic and smectic phases in two dimensions can only possess quasi-long-range order.

In 1971, McMillan used a simple molecular model to extend the Maier-Saupe model of the transition from the nematic phase to the smectic-A phase in the bulk (three dimensions). Here, we study the consequences of applying his approach in two

dimensions.

In this case, the appropriate order parameter for the nematic phase is $S = \langle \cos(2\theta) \rangle$, where θ is the angle between the long axis of the molecule and a preferred axis or director (taken as the z direction for convenience) in two-dimensional space. Similarly to the form proposed by McMillan [151], the anisotropic part of the pair potential, assuming an angle-independent uniform distribution of intermolecular distances, can be written as:

$$V_{12}(r_{12}, \cos \theta_{12}) = -(V_0/N\pi r_0^2) e^{-(r_{12}/r_0)^2} \cos(2\theta_{12}), \quad (4.1)$$

where r_{12} is the distance between the molecules' centers-of-mass, r_0 is of the order of the rigid core length of the molecule, and θ_{12} is the angle between the long axes of the two molecules.

To induce a smectic phase, we suppose that there is a density wave with a wavevector q_0 parallel to the director. This implies that we must expand $e^{-(z/r_0)^2}$ in terms of its Fourier components. Neglecting the terms higher than first-order, we obtain

$$e^{-z^2/r_0^2} = \sqrt{\pi} \left(\frac{r_0}{2d} \right) [1 + \zeta \cos(q_0 z)], \quad (4.2)$$

where $\zeta = 2 \exp[-(\pi r_0/d)^2] \text{erf}(d/r_0)$, with $q_0 = 2\pi/d$, and erf is the error function. ζ is a measure of the strength of the short-range interactions. Large values of ζ correspond to a strong attraction between the smectic layers.

The one-particle mean-field potential that a molecule feels is

$$V_1(z, \theta) = -V_0[S + \sigma\zeta \cos(2\pi z/d)] \cos(2\theta), \quad (4.3)$$

where σ is the smectic-phase order parameter controlling the amplitude and phase of the density wave along the z direction. An alternative way to express V_1 is through the pair interaction potential Eq.(4.1) using the one-particle distribution function $f_1(z, \theta) = \exp[-V_1(z, \theta)/k_B T]$. To this end, we have

$$V_1(z_1, \theta_1) = \frac{N \int d^2 \mathbf{r}_2 V_{12}(r_{12}, \cos \theta_{12}) f(z_2, \cos \theta_2)}{\int d^2 \mathbf{r}_2 f(z_2, \cos \theta_2)}. \quad (4.4)$$

In order for Eq.(4.3) and Eq.(4.4) to be self-consistent, we must require that

$$S = \langle \cos(2\theta) \rangle_f, \quad (4.5)$$

and

$$\sigma = \langle \cos(2\pi z/d) \cos(2\theta) \rangle_f, \quad (4.6)$$

where the average of a function O of z and θ is defined by

$$\langle O(z, \theta) \rangle_f = \frac{\int_0^d dz \int_0^{2\pi} d\theta O(z, \theta) f(z, \theta)}{\int_0^d dz \int_0^{2\pi} d\theta f(z, \theta)}. \quad (4.7)$$

In order to solve this set of equations, we first find the isotropic-nematic (N-I) transition temperature T_{NI} , which serves as the scale of temperature. At the N-I transition, σ becomes identically equal to zero, and therefore S is given by

$$S = \frac{\int_0^{2\pi} \exp[V_0 S \cos(2\theta)/k_B T] \cos(2\theta) d\theta}{\int_0^{2\pi} \exp[V_0 S \cos(2\theta)/k_B T] d\theta}. \quad (4.8)$$

If we let $a = V_0 S/k_B T$ and $x = \cos(2\theta)$, then S can be expressed as $S = d \ln I(a)/da$, with

$$I(a) = \int_{-1}^1 \frac{2e^{ax}}{\sqrt{1-x^2}} dx. \quad (4.9)$$

Solving for S numerically shows that the maximum temperature leading to a nonzero S , i.e., the N-I transition temperature T_{NI} , is $V_0/2k_B$, at which $S \approx 0.2$. Next, the set of self-consistent equations is solved by fixing a value for σ/\tilde{T} , where $\tilde{T} = T/T_{\text{NI}}$ is the reduced temperature. Then, choosing a trial value of S/\tilde{T} , Eq.(4.6) is used to determine \tilde{T} . However, this choice does not satisfy Eq.(4.5). Thus, we continue the trial procedure until we find a value of S/\tilde{T} which satisfies Eq.(4.5). At that point, we have the values of both order parameters at the same temperature. This procedure is repeated to establish S and σ as functions of temperature.

When the transition is first-order, i.e., when there is a discontinuity in the order parameter, we must compute the free energies of the two phases to determine which one is more stable. Similarly to the three-dimensional version of the theory, the Helmholtz free energy is given by

$$F = \frac{1}{2}NV_0(S^2 + \zeta\sigma^2) - Nk_B T \ln \mathcal{Z} , \quad (4.10)$$

where \mathcal{Z} is the one-particle partition function

$$\mathcal{Z} = d^{-1} \int_0^d dz \int_0^{2\pi} d\theta f(z, \theta) . \quad (4.11)$$

This model exhibits three distinct phases:

- (1) isotopic liquid ($S = 0, \sigma = 0$)
- (2) nematic ($S \neq 0, \sigma = 0$)
- (3) smectic-A ($S \neq 0, \sigma \neq 0$).

The behavior of the order parameters as functions of temperature depends on the value of ζ . For $\zeta < 1.54$ and $\tilde{T} < 0.88$, the smectic-A order parameter decreases

continuously to zero, and thus there is a second-order smectic-A - nematic (S-N) transition, followed by a first-order nematic-isotropic (N-I) transition at higher temperatures. For $1.54 < \zeta < 2$, σ drops discontinuously to zero, i.e., the S-N transition is first-order, and since the nematic and smectic-A order parameters are coupled, there is also an abrupt change in S to a nonzero value. S will eventually vanish at $\tilde{T} = 1$. Therefore, $\zeta = 1.54$ and $\tilde{T}_{SN} = 0.88$ correspond to a tricritical point, at which the line of first-order transitions goes over to a line of second-order transitions. Finally, at $\zeta = 2$, which is the maximum value the interaction parameter can adopt, both order parameters go to zero at $\tilde{T} = 1$. The variations of the order parameters with temperature at two values of ζ are shown in Fig.4.8 and Fig.4.9.

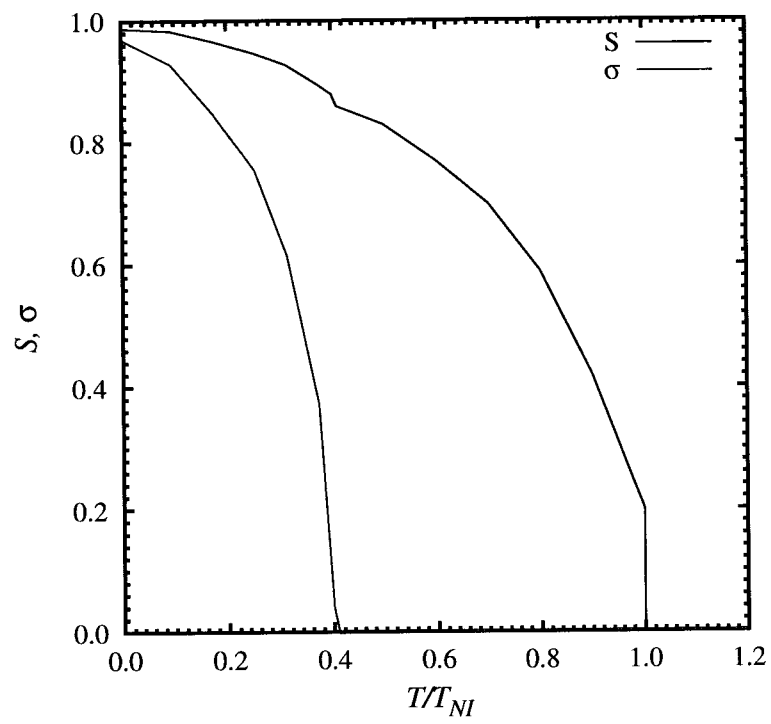


Figure 4.8: Order parameters S and σ as functions of reduced temperature for $\zeta = 0.5$.

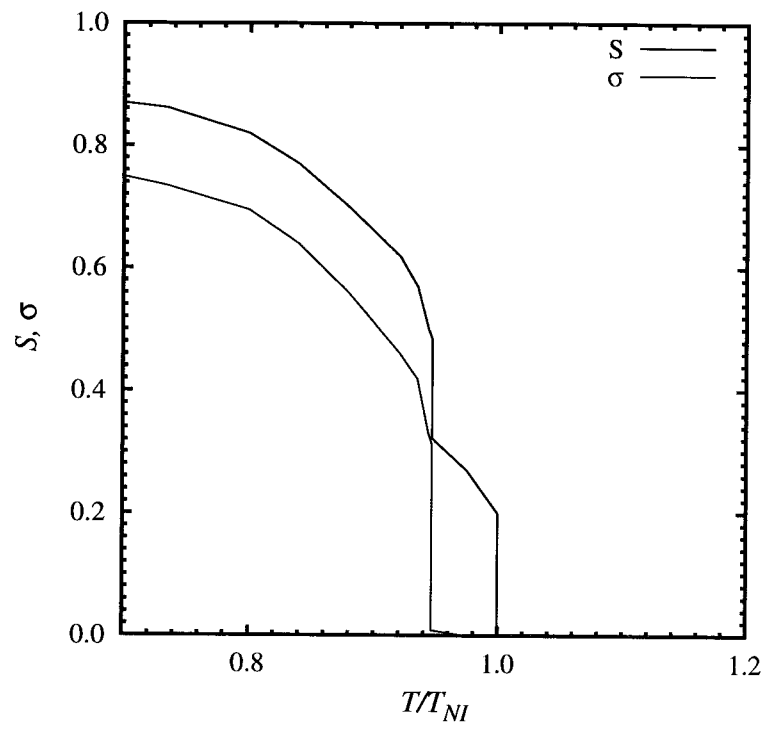


Figure 4.9: Order parameters S and σ as functions of reduced temperature for $\zeta = 1.8$.

The major qualitative difference between the two-dimensional and three-dimensional versions of McMillan's theory is that in two dimensions, except in the limiting case of $\zeta = 2$, the smectic-A phase does not melt directly into the isotropic phase. From a quantitative point of view, the nematic order parameter has a lower value at the N-I transition compared to that of the three-dimensional case where $S_{NI} = 0.43$. Also, the tricritical point occurs at a higher value of the interaction parameter. These results can be regarded as a consequence of the fact that there are fewer immediate neighbors that a given molecule can interact with when we reduce the dimensionality, leading to a weaker mean-field potential (if everything else is left unchanged).

The effect of the concentration of the molecules is contained in V_0 . V_0 increases with increasing concentration, and this shifts the transition temperatures to higher values. It is worth mentioning that the original formulation of Maier and Saupe displays a ρ^2 dependence of V_0 , whereas Cotter [152] demonstrated subsequently that thermodynamic consistency requires V_0 to be proportional to ρ , regardless of the nature of the intermolecular pair potential.

As opposed to its original version in three dimensions, McMillan's model in two dimensions does not allow for a direct transition from the isotropic phase to the smectic-A phase, i.e., the former always goes through a nematic phase. Therefore, unless the nematic phase is missed in the experiments, this model is not capable of explaining the experimental results.

Chapter 5

Future Studies

Many interesting and challenging questions regarding diffusion and phase transitions in confined colloid-polymer mixture are raised by this research. Here, we describe some of them and propose possible directions for finding answers.

Microfluidics and Non-equilibrium Phase Transitions

In studying the diffusion of confined colloid-polymer mixtures, our focus has been on the dynamics in the absence of any external flow field. In other words, the fluid was initially quiescent, with no preferred direction for the motion of particles. It would be of interest to investigate the effect of a flow induced by an external field (a pressure-driven flow for example) on the transport properties of the mixture. It is not obvious if the drift of the particles due to the flow is merely an additive contribution to the total dispersion coefficient (the other part coming from purely diffusive

motions). Indeed the particles, if they are large enough, do not necessarily follow the streamlines. In fact, the streamlines are perturbed in the vicinity of the particles. It is also known that at sufficiently high velocities, the structure of polymers around a moving colloid is very different from their structure in the case of vanishing Reynolds number [153]. In addition, the problem of dynamic phase transitions that can occur under such non-equilibrium conditions is an interesting one to investigate.

Beyond the Asakura-Oosawa Model

While the Asakura-Oosawa model enables one to perform analytic calculations, it is not reliable quantitatively [52], in particular at high concentrations, mainly because of its neglect of the polymer internal structure. More realistic models are called for in order to address dynamics in the concentrated regime, and possibly to include other types of interactions such as electrostatic repulsion between charged particles or polymers. However, such models are difficult to treat analytically. Perhaps computer simulations could shed light on this problem.

Crossover From One to Two Dimensions

In this thesis, we considered the diffusion in a one-dimensional geometry. The crossover to two dimensions and the diffusion in two-dimensional geometry is yet to be investigated theoretically, and comparison should be made with earlier experimental results obtained in our group [126]. Determination of the exact value of the

critical radius (or width) of the channel, at which the crossover to two dimensions occurs, calls for a generalized description of hydrodynamic interactions in order to yield a smooth transition from one to two dimensions. The results may also depend on the stiffness of the polymer, which is characterized by its persistence length.

Long-time Diffusion

A complete description of the diffusion in colloid-polymer mixtures with colloid and polymer of arbitrary size ratio, and at all accessible time scales, involves the consideration of coupled dynamics of colloidal particles and polymer chains. The major challenge to tackle this problem, apart from the many-body interactions, is the existence of multiple relevant length and time scales in the system. Analytical calculations are thus very difficult (although renormalization concept may prove useful). One way to tackle this problem is to employ computer simulation techniques such as Brownian dynamics, coupled to fast numerical algorithms, in order to solve the hydrodynamic equations. However, these calculations, even for the coarse-grained models of a single DNA molecule in a microchannel with no particles, require significant computer resources.

Correlations in Two-Dimensional Liquid Crystals

It is not clear whether the observed isotropic to smectic-A transition in PLA monolayers is of the Kosterlitz-Thouless type or not. To elucidate that point, the

orientational correlations in the ordered (smectic-A) phase have to be determined. The algebraic decay of these correlations with distance is a signature of the Kosterlitz-Thouless transition. As a corollary, the isothermal compressibility of the smectic phase diverges at and below the Kosterlitz-Thouless transition temperature.

A related future study is that of the microstructures of PLA-particle mixtures. In this regard, Brewster-angle microscopy (BAM) and atomic force microscopy (AFM) are capable to shed light on the arrangement of magnetic colloids and nanoparticles in the PLA-particle mixtures.

It is also of interest to examine the phase behavior and correlations in systems consisting of charged species or subject to external fields. In this respect, a natural extension of our studies is to apply an external magnetic field, so that superparamagnetic colloids acquire dipole moments whose strength can be readily tuned by varying the intensity of the external magnetic field.

Bibliography

- [1] L.D. Gelb, K.E. Gubbins, R. Radhakrishnan, and M. Silwinska-Bartkowiak. *Rep. Prog. Phys.*, 62:1573, 1999.
- [2] K. Zahn, J.M. Méndez-Alcaez, and G. Maret. *Phys. Rev. Lett.*, 79:175, 1997.
- [3] J.A. Lewis. *J. Am. Ceram. Soc.*, 83:2341, 2000.
- [4] P. Jiang, J.F. Bertone, K.S. Hwang, and V.L. Colvin. *Chem. Mater.*, 11:2132, 1999.
- [5] P. Jiang, J.F. Bertone, and V.L. Colvin. *Science*, 291:453, 2001.
- [6] R. Rengarajan, P. Jiang, V. Colvin, and D. Mittleman. *Appl. Phys. Lett.*, 77:3517, 2000.
- [7] P. Subramanian, V.N. Manoharan, J.D. Thorne, and D.J. Pine. *Adv. Mater.*, 11:1261, 1999.
- [8] Y. Lu, Y. Yin, and Y. Xia. *Langmuir*, 17:6344, 2001.
- [9] A.V. Petukhov, D.G.A.L. Aarts, I.P. Dolbnya, E.H.A. de Hoog, K. Kassapidou, G.J. Vroege, W. Bras, and H.N.W. Lekkerkerker. *Phys. Rev. Lett.*, 88:208301–1, 2002.
- [10] O.D. Velev, P.M. Tessier, A.M. Lenhoff, and E.W. Kaler. *Nature*, 401:548, 1999.
- [11] P.S. Doyle, J. Bibette, A. Bancaud, and J.L. Viovy. *Science*, 295:227, 2002.
- [12] J. Bibette, F. Leal Calderon, V. Schmitt, and P. Poulin. *Emulsion Science: Basic Principles, an Overview*. Springer Verlag, 2002.
- [13] J.E. Smay, J. Cesarano, and J.A. Lewis. *Langmuir*, 18:5429, 2002.
- [14] A.D. Dinsmore, M.F. Hsu, M.G. Nikolaides, M. Marquez, A.R. Barsch, and D.A. Weitz. *Science*, 298:1006, 2002.
- [15] W.B. Russel, D.A. Saville, and W.R. Schowalter. *Colloidal Dispersions*. Cambridge University Press, Cambridge, 1989.

- [16] J. Kärger and D.M. Ruthven. *Diffusion in Zeolites and Other Microporous Solids*. Wiley, New York, 1992.
- [17] N.Y. Chen, T.F. Degnan, and C.H. Smith. *Molecular Transport and Reaction in Zeolites*. VCH, New York, 1994.
- [18] D.G. Levitt. *Biochem. Biophys. Acta*, 373:115, 1974.
- [19] J.A. Hernandez and J. Fischberg. *J. Gen. Physiol*, 99:645, 1992.
- [20] T. Chou and D. Lohse. *Phys. Rev. Lett.*, 82:3552, 1999.
- [21] B. Lin, J. Yu, and S.A. Rice. *Phys. Rev. E*, 62:3909, 2000.
- [22] P.A. Kralchevsky and K. Nagayam. *Particles at Fluid Interfaces and Membranes*, chapter 13. Elsevier, Amsterdam, 2001.
- [23] R. Tuinier and H.N.W. Lekkerkerker. *Macromolecules*, 35:3312, 2002.
- [24] R.B. Bird, W.E. Stewart, and E.N. Lightfoot. *Transport Phenomena*, pages 514–533.
- [25] E.G.D. Cohen, R. Verberg, and I.M. de Schepper. *Physica A*, 251:251, 1998.
- [26] G. Nägele and J.K.G. Dhont. *J. Chem. Phys.*, 108:9566, 1998.
- [27] A.J.C. Ladd, H. Gang, J.X. Zhu, and D.A. Weitz. *Phys. Rev. Lett.*, 74:318, 1995.
- [28] D.R. Foss and J.F. Brady. *J. Rheol.*, 44:629, 2000.
- [29] R. Verberg, I.M. de Schepper, and E.G.D. Cohen. *Phys. Rev. E*, 61:2967, 2000.
- [30] A. Kasper, E. Bartsch, and H. Sillescu. *Langmuir*, 14:5004, 1998.
- [31] E.R. Weeks and D.A. Weitz. *Phys. Rev. Lett.*, 89:095704–1, 2002.
- [32] E.R. Weeks and D.A. Weitz. *J. Chem. Phys.*, 284:361, 2002.
- [33] H. van Beijeren, K.W. Kehr, and R. Kutner. *Phys. Rev. B*, 28:5711, 1983.
- [34] Q.-H. Wei, C. Bechinger, and P. Leiderer. *Science*, 287:625, 2000.
- [35] K. Hahn and J. Kärger. *J. Phys. Chem. B.*, 102:5766, 1998.
- [36] C. Bechinger. *Curr. Opin. Colloid Interface Sci.*, 7:204, 2002.
- [37] B. Lin, B. Cui, J.-H Lee, and J. Yu. *Europhys. Lett.*, 57:724, 2002.

- [38] H. Löwen. *J. Phys.: Condens. Matter*, 13:R415, 2001.
- [39] P.-G. de Gennes. *Introduction to Polymer Dynamics*. Cambridge University Press, 1990.
- [40] M. Doi and S.F. Edwards. *The Theory of Polymer Dynamics*. Oxford Science Pub., 1986.
- [41] D.E. Smith, T.T. Perkind, and S. Chu. *Phys. Rev. Lett.*, 75:4146, 1995.
- [42] B. Maier and J.O. Rädler. *Phys. Rev. Lett.*, 82:1911, 1999.
- [43] B. Maier and J.O. Rädler. *Macromolecules*, 33:7185, 2000.
- [44] T. Kuhlmann, J. Kraus, P. Muller-Buschbaum, D.W. Schubert, and M. Stamm. *J. Non-Crystalline Solids*, 457:235, 1998.
- [45] F. Brochard Wyart and P.-G. de Gennes. *Euro. Phys. J. E.*, 1:93, 2000.
- [46] J.-T. Lee. PhD thesis, Rice University, 2000.
- [47] T.-C. Lee. PhD thesis, Rice University, 2002.
- [48] T.-C. Lee, J.-T. Lee, D.R. Pilaski, and M. Robert. *Physica A*, page 431, 2003.
- [49] P.-G. de Gennes. *Scaling Concepts in Polymer Physics*. Cornell University Press, Ithaca, 1979.
- [50] R.L.C. Vink and M. Schmidt. *Phys. Rev. E*, 71:051406, 2005.
- [51] J.-T. Lee and M. Robert. *Phys. Rev. E*, 60:7198, 1999.
- [52] C.-Y. Chou, T.T.M Vo, A.Z. Panagiotopoulos, and M. Robert. *Physica A*, 369:275, 2006.
- [53] A. Fortini, M. Schmidt, and M. Dijkstra. *Phys. Rev. E*, 73:051502, 2006.
- [54] R.L.C. Vink, A. De Virgiliis, J. Horbach, and K. Binder. *Phys. Rev. E*, 74:031601, 2006.
- [55] R.H.G Brinkhuis and A.J. Schouten. *Macromolecules.*, 24:1487, 1991.
- [56] D.J. Crisp. *J. Colloid Sci.*, 1:49, 1946.
- [57] D.J. Crisp. *J. Colloid Sci.*, 1:161, 1946.
- [58] A. Labbauf and J.R. Zack. *J. Colloid Interf. Sci.*, 35:569, 1971.

- [59] P. Stroeve, M.P. Srinivasan, B.G. Higgins, and S.T. Kowel. *Thin Solid Films*, 146:209, 1987.
- [60] P. Baglioni, F. Dei, and M. Puggelli. *J. Colloid Interf. Sci.*, 283:266, 1985.
- [61] G. Gabrielli, M. Puggelli, and Faccioli R. *J. Colloid Interf. Sci.*, 11:63, 1972.
- [62] G. Gabrielli, M. Puggelli, and P. Baglioni. *J. Colloid Interf. Sci.*, 86:485, 1982.
- [63] S.W. Kuan, C.W. Frank, C.C. Fu, D.R. Allee, P. Maccagno, and R.F.W. Pease. *J. Vac. Sci. Technol. B*, 6:2274, 1988.
- [64] B.B. Sauer, H. Yu, M. Yazdanian, G. Zograf, and M.W. Kim. *Macromolecules*, 22:2332, 1989.
- [65] M Kawaguchi, B.B. Sauer, and Y. Hyuk. *Macromolecules*, 22:1735, 1981.
- [66] N. Bredjik, R.A. Ahlbeck, T.K. Kwei, and H.E. Ries Jr. *J. Polym. Sci.*, 46:268, 1960.
- [67] N. Bredjik and H.E. Ries Jr. *J. Polym. Sci.*, 62:864, 1962.
- [68] M.M. Dovek, T.R. Albercht, S.W.J. Kuan, C.A. Lang, R. Emch, P. Grütter, C.W. Frank, R.F.W. Pease, and C.F. Quate. *J. Microsc. (Oxford)*, 152:229, 1988.
- [69] T.R. Albercht, M.M. Dovk, C.A. Lang, Grütter P., C.F. Quate, Kuan S.W.J., C.W. Frank, and Pease R.F.W. *J. Appl. Phys.*, 64:1178, 1988.
- [70] S.W.J. Kuan, P.S. Martin, C.W. Frank, and R.F.W. Pease. *Polym. Mater. Sci. Eng.*, 60:270, 1989.
- [71] M. Oettel. *Phys. Rev. E*, 76:041403, 2007.
- [72] Dominguez A., M. Oettel, and S. Dietrich. *J. Phys. Condens. Matter*, 17:S3387, 2005.
- [73] P. Pieranski. *Phys. Rev. Lett.*, 45:569, 1980.
- [74] B.-J. Lin and Chen L.-J. *J. Chem. Phys.*, 126:034706, 2007.
- [75] R. Aveyard, B.P. Binks, J.H. Clint, P.D.I. Fletcher, T.S. Horozov, B. Neumann, V.N. Paunov, J. Annelsey, S.W. Botchway, D. Nees, A.W. Parker, A.D. Ward, and A.N. Burgess. *Phys. Rev. Lett.*, 88:246102, 2002.
- [76] M.G. Nikolaidis, A.R. Bausch, M.F. Hsu, A.D. Dinsmore, M.P. Brenner, C. Gay, and D.A. Weitz. *Nature*, 420:299, 2002.

- [77] E. Worlet, S.M. Setz, R.S. Underhill, R.S. Duran, M. Schappacher, A. Deffieux, M. Hölderle, and R. Mülhaupt. *Langmuir*, 17:5671, 2001.
- [78] E. Rukenstein and B. Li. *J. Phys. Chem. B*, 102:981, 1998.
- [79] J. Sun and T. Stirner. *J. Chem. Phys.*, 121:4292, 2004.
- [80] N.I.D Fenwick, F. Bresme, and N. Quirke. *J. Chem. Phys.*, 114:7274, 2001.
- [81] M. Suzuki, M. Kakimoto, T. Konishi, Y. Imai, M. Iwamoto, and T. Hino. *Chem. Lett.*, page 395, 1986.
- [82] M. Era, K. Kamiyama, K. Yoshimura, T. Momii, H. Murata, S. Tokito, T. Tsutsui, and S. Saito. *Thin Solid Films*, 179:1, 1989.
- [83] A.R. Esker, C. Kim, and H. Yu. *Adv. Polym. Sci.*, 209:59, 2007.
- [84] A.C. Nieuwkerk, E.J.M. van Ken, P. Kimkes, A.T.M. Marcelis, and E.R.J. Sudhölter. *Langmuir*, 14:6448, 1998.
- [85] G. Nägele. *Physics Reports*, 272:215, 1996.
- [86] J.K.G. Dhont. *An Introduction to Dynamics of Colloids*. Elsevier, Amsterdam, 1996.
- [87] R. Zwanzig. *Adv. Chem. Phys.*, 15:325, 1969.
- [88] R. Verberg, I.M. de Schepper, and E.G.D. Cohen. *Phys. Rev. E*, 61:2967, 2000.
- [89] D. Forster. *Hydrodynamic Fluctuations, Broken Symmetry, and Correlation Functions*. Addison Wesley, 1990.
- [90] J.P. Hansen, D. Levesque, and J. Zinn-Justin, editors. *Liquids, Freezing and the Glass Transition*. North-Holland, 1991.
- [91] J.P. Boon and S. Yip. *Molecular Hydrodynamics*. Courier Dover Publications, 1992.
- [92] G.K. Batchelor. *J. Fluid Mech.*, 74:1, 1976.
- [93] W. Hess and R. Klein. *Adv. Phys.*, 32:173, 1983.
- [94] G. Nägele, T. Zwick, R. Krause, and R. Klein. *J. Colloid Interface Sci.*, 161:347, 1993.
- [95] H. Mori. *Prog. Theor. Phys.*, 34:399, 1965.
- [96] L. Onsager. *Phys. Rev.*, 37:405, 1931.

- [97] L. Onsager. *Phys. Rev.*, 38:2265, 1931.
- [98] B. Lin, M. Meron, B. Cui, S.A. Rice, and H. Diamant. *Phys. Rev. Lett.*, 94:216001, 2005.
- [99] T.E. Harris. *J. Appl. Prob.*, 2:323, 1965.
- [100] J. Kärger. *Phys. Rev. A*, 45:4173, 1992.
- [101] J. Kärger. *Phys. Rev. E*, 47:1427, 1993.
- [102] C.Y. Chou, B.C. Eng., and M. Robert. *J. Chem. Phys.*, 124:044902–1, 2006.
- [103] M. Kollmann. *Phys. Rev. Lett.*, 90:180602, 2003.
- [104] B. Cui, H. Diamant, and B. Lin. *Phys. Rev. Lett.*, 89:188302, 2002.
- [105] J. Hapel and H. Brenner. *Low Reynolds Number Hydrodynamics*. Martinus Nijhoff, Dordrecht, 1983.
- [106] E.R. Dufresne, T.M. Squires, M.P. Brenner, and D.G. Grier. *Phys. Rev. Lett.*, 85:3317, 2000.
- [107] C. Pozrikidis. *Boundary Integral and Singularity Methods for Linearized Viscous Flow*. Cambridge University Press, New York, 1992.
- [108] N. Liron and S. Mochon. *J. Eng. Math.*, 10:287, 1976.
- [109] N. Liron and S. Shahar. *J. Fluid Mech.*, 86:727, 1978.
- [110] J.R. Blake. *J. Fluid Mech.*, 95:209, 1979.
- [111] X. Xu and S.A. Rice. *J. Chem. Phys.*, 122:024907, 2005.
- [112] X. Xu, S.A. Rice, B. Lin, and H. Diamant. *Phys. Rev. Lett.*, 95:158301, 2005.
- [113] Z.W. Salsburg, R.W. Zwanzig, and J.G. Kirkwood. *J. Chem Phys.*, 21:1098, 1953.
- [114] L. Binhua, J. Yu, and S.A. Rice. *J. Chem Phys.*, 62:3909, 2000.
- [115] S. Asakura and F. Oosawa. *J. Chem. Phys.*, 22:1255, 1954.
- [116] A. Vrij. *Pure Appl. Chem.*, 48:471, 1976.
- [117] A.P. Gast, C.K. Hall, and W.B. Russel. *J. Colloid Interface Sci.*, 96:251, 1983.
- [118] M. Dijkstra, J.M. Brader, and R. Evans. *J. Phys.: Condens. Matter*, 11:10079, 1999.

- [119] M. Dijkstra, R. van Roij, and R. Evans. *J. Chem. Phys.*, 113:4799, 2000.
- [120] H.N.W. Lekkerkerker and B. Widom. *J. Stat. Phys.*, 285:483, 2000.
- [121] J.M. Brader and R. Evans. *Physica A*, 306:287, 2002.
- [122] S. Asakura and F. Oosawa. *J. Polym. Sci.*, 33:183, 1958.
- [123] H. Hansen-Goos, C. Lutz, C. Bechinger, and R. Roth. *Europhys. Lett.*, 74:8, 2006.
- [124] T.T.M. Vo, L.-J. Chen, and M. Robert. *J. Chem. Phys.*, 119:5607, 2003.
- [125] T.-H. Fan, J.K.G. Dhont, and R. Tuinier. *Phys. Rev. E*, 75:011803, 2007.
- [126] C.-Y. Chou. PhD thesis, Rice University, 2004.
- [127] J.G. Kirkwood and J. Riseman. *J. Chem. Phys.*, 16:565, 1948.
- [128] B.H. Zimm. *J. Chem. Phys.*, 24:269, 1956.
- [129] M. Fixman. *J. Chem. Phys.*, 45:793, 1966.
- [130] M. Fixman. *J. Chem. Phys.*, 61:4939, 4950, 1974.
- [131] J.L. Harden and M. Doi. *J. Phys. Chem.*, 96:4046, 1992.
- [132] E.A. DiMarzio. *J. Chem. Phys.*, 42:2101, 1965.
- [133] E.F. Casassa. *Macromolecules*, 17:60, 1984.
- [134] R.J. Gaylord and D.J. Lohse. *J. Chem. Phys.*, 65:2279, 1976.
- [135] B. Gidas, W. Ni, and L. Nirenberg. *Commun. Math. Phys.*, 68:209, 1979.
- [136] F. Brochard and P.-G. de Gennes. *J. Chem. Phys.*, 67:52, 1977.
- [137] D.S. Cannell and F. Rondelez. *Macromolecules*, 13:1599, 1980.
- [138] J. Des Cloizeaux and G. Jannink. *Polymers in Solution: Their Modelling and Structure*. Oxford University Press, Oxford, U.K., 1989.
- [139] H.P. Gillis and K.F. Freed. *J. Chem. Phys.*, 63:852, 1975.
- [140] K. Kremer and K. Binder. *J. chem. Phys.*, 81:6381, 1984.
- [141] H. Reiss, H.L. Frisch, and J.L. Lebowitz. *J. Chem. Phys.*, 31:369, 1959.
- [142] H. Bourque, L. Laurin, M. Pezolet, J.M. Klass, R.B. Lennox, and G.R. Brown. *Langmuir*, 17:5842, 2001.

- [143] L. Pelletier and M. Pezolet. *Macromolecules*, 37:4967, 2004.
- [144] S. Ni, W. Lee, B. Li, and A.R. Esker. *Langmuir*, 22:3672, 2006.
- [145] S. Ni, W. Yin, M.K. Ferguson-McPherson, S.K. Satija, J.R. Morris, and A.R. Esker. *Langmuir*, 22:5969, 2006.
- [146] R.L.C. Vink. *Phys. Rev. Lett.*, 98:217801, 2007.
- [147] D.G.A.L. Aarts and H.N.W. Lekkerkerker. *J. Phys.: Condens. Matter*, 16:S4231, 2004.
- [148] M.A. Cotter. *Phys. Rev. A*, 4:675, 1971.
- [149] M.A. Bates and D. Frenkel. *J. Chem. Phys.*, 112:10034, 2000.
- [150] N.D. Mermin. *Phys. Rev.*, 250:176, 1968.
- [151] W.L. McMillan. *Phys. Rev. A*, 4:1238, 1971.
- [152] M.A. Cotter. *Mol. Cryst. Liquid Cryst.*, 39:173, 1977.
- [153] C. Gutsche, F. Kremer, M. Krüger, and M. Rauscher. *J. Chem. Phys.*, 129:084902, 2008.